Entropy Analysis of Maxwell Nanofluid with Thermal Radiation and Viscous Dissipation

By

Tayyaba Mukhtar

Regn.#203314

A dissertation submitted in partial fulfillment of the requirements for

the degree of Master of Sciences in Mathematics

Supervised by : Dr. Asim Aziz

DEPARTMENT OF MATHEMATICS,
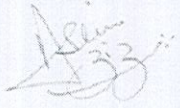
SCHOOL OF NATURAL SCIENCES,

NATIONAL UNIVERSITY OF SCIENCES AND TECHNOLOGY

ISLAMABAD, PAKISTAN

National University of Sciences & Technology

MS THESIS WORK

We hereby recommend that the dissertation prepared under our supervision by: TAYYABA MUKHTAR, Regn No. 00000203314 Titled: Entropy Analysis of Maxwell Nanofluid with Thermal Radiation and Viscous Dissipation accepted in partial fulfillment of the requirements for the award of **MS** degree.

Examination Committee Members

1. Name: DR. MUHAMMAD ASIF FAROOQ   Signature: _____

2. Name: DR. SYED TAYYAB HUSSAIN   Signature: _____

External Examiner: DR. REHMAT ELLAHI   Signature: _____

Supervisor's Name DR. ASIM AZIZ   Signature: _____
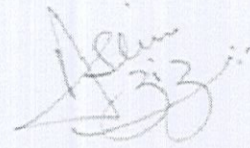   Dr. Asim Aziz

_____
Head of Department

15 - 07 - 2020
Date

COUNTERSINGED

Date: 21/7/2020

Dean/Principal

THESIS ACCEPTANCE CERTIFICATE

Certified that final copy of MS thesis written by **Ms. Tayyaba Mukhtar** (Registration No. **00000203314**), of **School of Natural Sciences** has been vetted by undersigned, found complete in all respects as per NUST statutes/regulations, is free of plagiarism, errors, and mistakes and is accepted as partial fulfillment for award of MS/M.Phil degree. It is further certified that necessary amendments as pointed out by GEC members and external examiner of the scholar have also been incorporated in the said thesis.

Dr. Asim Aziz

Signature: _____

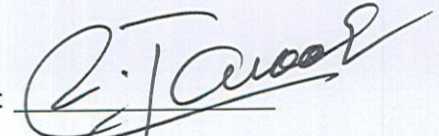Name of Supervisor: Dr. Asim Aziz

Date: _____ 30-6-2020 _____

Signature (HoD): _____

Date: 15 - 07 - 2020

Signature (Dean/Principal): _____

Date: 21/7/2020

Dedicated

to

My Beloved Parents

ACKNOWLEDGMENTS

Abstract

In this dissertation, heat transfer and entropy of an unsteady non-Newtonian Maxwell nanofluid flow is studied. The fluid is positioned over a flat stretching sheet being stretched with non-uniform velocity. The study of nanofluid flow and heat transfer is presented under the influence of partial slip and convective boundary conditions. The effects of thermal radiation and viscous dissipation along with magnetohydrodynamics are considered. The governing partial differential equations for current model are obtained by using boundary layer approximations, reduced into ordinary differential equations using similarity transformation and then the numerical results of ordinary differential equations are computed for Copper water and Titanium water nanofluids by using Keller box method. The effects of various governing flow parameters on fluid movement, temperature difference, entropy of system, skin friction and nusselt number near the boundary are discussed.

Contents

Chapter 1

Introduction

The study of nanofluid flow and heat transfer has gained importance in current era due to its significant importance in engineering applications. Nanofluids are used in many processes, nanofluids act as coolant in many industrial cooling applications and used in oil extraction process, computer processors, thermal solar collectors, radiator etc. Nanofluids are obtained by the dispersion of nanoparticles in base fluid. Nanofluids enhanced the heat transfer characteristics of ordinary fluids. Choi and Eastman [1]- [3] at first introduce the idea of dispersion of nanoparticles in base fluid to enhance the thermal conductivity. Different materials such as metals $(Al; Cu)$, carbides (S_iC) or oxides (Al_2O_3) are used as nanoparticles and usually a conductive fluid such as water and ethylene glycol is used as a base fluid. Experimental study revealed that the thermal conductivity of nanofluids varies as concentration, size, shape and material of the nanoparticles changes (Lomascolo et al. [4]). Enhancement of thermal conductivity is in fact based on nanoparticles but the enhancement and effectiveness of heat transfer depends upon the material type and shape of particles dispersed.

The study of nanofluids over stretching surface is an interesting part of discussion. The idea of boundary layer flow over a stretching surface was initiated by Sakiadis [5]. The study of natural convective flow has been receiving a great attention in recent years based on various applications in many fields of engineering including cooling devices, thermoelastic damping, thermal flow in boiler tubes etc. The connection of normal convection with thermal radiation is expanded incredibly in the most recent decade because of its significance in numerous handy contributions. Thermal radiation perform a vital role in nuclear power plants, aerothermodynamics and furnace operations. The analysis of effects of heat absorption and generation is very important in cooling processes. Navier-Stokes equations are used to study Newtonian fluids but some of the fluids in the industry have different rheological properties like toothpaste, paint, alloys etc. It is important to mention here that some practical applications where the significant temperature distribution between the surface of the body and the temperature at infinity exists. There may be some buoyancy forces due to natural convection and the heat transfer distribution determined by two setups namely, the movement of stretching sheet and the gravitational effects. The thermal buoyancy is produced due to the heating cooling of a vertical movement of stretching sheet that has large influence on the flow and heat transfer mechanism.

An unsteady MHD flow, heat and mass transfer over a horizontal stretching sheet in the presence of heat generation/absorption was discussed by Mukhopadhyay [6]. By applying the uniform stress, the sheet bears an incompressible flow which was first studied by Crane [7]. Ishak *et al.* [8] discussed the MHD flow through a stretched sheet by using the Keller box method. The slip effect was firstly introduced by Dorrepaal [9]. Noghrehabadi *et al.* [10] investigated the effect of partial slip condition

2

on heat transfer rate of nanofluids over a stretching sheet. Sharma *et al.* [11] investigated the slip effect of a CuO- water nanofluid on heat transfer rate over stretching sheet. Although, the effects of viscous dissipation are negligible sometimes, but its effects are more significant when the fluid viscosity is very high. Magnetohydrodynamics (MHD) is the sequence of Navier-stokes equations and Maxwell equations of electromagnetism are discussed by Chakraborty *et al.* [12]. Entropy is a thermodynamic property, it can be viewed as a measure of disorder. A. Aziz *et. al* [13] examined the impact of partial slip and convective conditions on Maxwell nanofluid over a stretching sheet by using Keller box Method. The entropy generation is correlated to a heat transfer, magnetic field, viscous dissipation, heat and mass transfer. Researchers used the second law of thermodynamics in different problems [14]- [16].

The main purpose of present analysis is to study the unsteady two-dimensional boundary layer flow of Maxwell nanofluid due to non-uniform velocity of stretching sheet. In this reference the findings of the work done by A. Aziz *et al.* [13] have been reproduced. Main fundamental partial differential equations are attained and transformed into non-linear and coupled ordinary differential equations by using a similarity transformation and in the end Keller box method is used to find the numerical solution of problem. Same model is then discussed under the effect of viscous dissipation and constant thermal conductivity but excluding porosity factor. The resulting equations are again transformed by means of similarity transformation and then solved numerically by Keller box numerical scheme. The effects of applied magnetic field are also included in this analysis. The main aim of this analysis is to numerically study the entropy generation thermal models of non-Newtonian nanofluids by taking convective conditions into account. Results are presented graphically and discussed qualitatively to illustrate the solution.

3

This thesis comprises of five chapters. Chapter 2 contains some important definitions and concepts which are used in subsequent chapters. Chapter 3 presents detailed numerical observation for two-dimensional, incompressible, laminar and unsteady flow of reviewed work. The numerical results are obtained, compared and found an excellent agreement with the published results of [13]. In Chapter 4, the nanofluid motion and temperature are analyzed for unsteady laminar flow under the effects of viscous dissipation and thermal radiation but neglecting the porosity effects. This chapter consists of partial differential equations governing the extended model, development of numerical solution and discussion of results. Dimensionless velocity and temperature gradient (Skin friction coefficient and Russell numbers) are also calculated at the boundary. Chapter 5 concludes the entire work and suggests the possible future work.

Chapter 2

Basic definitions

This Chapter covers, some basic laws, definitions, terminologies, and some classical methods for solving nonlinear pdes and odes would be described, which will be useful for the understanding of the subsequent chapters. The detailed discussion on basic law and definitions is given in [17].

2.1   Fluid

Fluid is a material which has no fixed shape and easily deforms when shear stress is applied.

2.2   Fluid flow

The random motion of a fluid is known as flow. Different flow types are given as follows.

2.2.1 Steady flow and Unsteady flow

In steady flow, fluid's properties does not alter with time. For such flows, one can write

$$\frac{d\zeta}{dt} = 0, \tag{2.1}$$

But if fluid at a particular time changes its properties is known as unsteady flow. Then

$$\frac{d\zeta}{dt} \neq 0, \tag{2.2}$$

where t is time and ζ is used to represent any fluid property.

2.2.2 Laminar flow and turbulent flow

Ordered movement of fluid particles in form of laminas or parallel smooth layers is knowm as laminar flow. This flow usually occurs while dealing with low Reynolds number. While in turbulent flow, the fluid particles movement is irregular and the path lines are the erratic curves. This type of flow occurs with high Reynolds number.

2.2.3 Compressible flow and incompressible flow

If in a fluid flow the density (ρ) with respect to the substance does not remains constant is said to be a compressible flow. Mathematically, it is expressed by

$$\frac{D\rho}{Dt} \neq 0. \tag{2.3}$$

But if density remains constant, is said to be an incompressible flow i.e.

$$\frac{D\rho}{Dt} = 0. \tag{2.4}$$

Here, $\frac{D}{Dt}$ represents material derivative.

2.2.4 Uniform flow and non-uniform flow

Uniform flow has constant magnitude and direction throughout the motion of a fluid.

$$\frac{dV}{ds} = 0, \tag{2.5}$$

Whereas in non-uniform flow, magnitude and direction changes during the motion of a fluid.

$$\frac{dV}{ds} \neq 0, \tag{2.6}$$

where V and s represent velocity and displacement respectively.

2.3 Stress

Stress is defined as the force (F) acting on the surface of the unit area (A) with in the distortable body. Mathematical expression of stress is

$$\tau = \frac{F}{A}. \tag{2.7}$$

where, τ is representation of stress.

2.4   Newtonian and non-Newtonian Fluids

The fluid is said to be Newtonian fluid if the stress arising from every point of flow is linearly proportional to the strain rate. The fluids for which the shear stress of the fluid varies directly and linearly as the deformation rate, are called Newtonian fluids. In other words, all those fluids which obey the Newton's law of viscosity are known as Newtonian fluids. Mathematically,

$$\tau = \mu \frac{du}{dy}, \tag{2.8}$$

Where μ presents viscosity, τ is the stress tensor, $\frac{du}{dy}$ denotes the deformation rate. Fluids are said to be non-Newtonian fluids for which the shear stress is not linearly proportional to the deformation rate. All those fluids which do not obey the Newton's law of viscosity are known as non-Newtonian fluids. For non-Newtonian fluids the relation between the shear stress and deformation rate of fluid is not linear. Mathematically,

$$\tau_{xy} = \mu \left[\frac{du}{dy} \right]^m, m \neq 1. \tag{2.9}$$

where μ is the apparent viscosity, m is the index of flow performance. where τ_{xy} is the shear stress, u denotes the velocity. Gasoline and water are particular examples of Newtonian fluids whereas toothpaste, blood, ketchup, drilling muds, biological fluids etc are non-Newtonian fluids.

2.5   Maxwell Fluid

Maxwell model proposed by James Clerk Maxwell in 1867. A Maxwell fluid is a viscoelastic material having the properties of both elasticity and viscosity.

2.6   Basic Equations

2.6.1   Continuity Equation

The continuity equation is based on law of conservation of mass which states that mass never changes inside the fixed control system. Mathematically, it is defined as

$$\frac{\partial \rho}{\partial t} + \nabla \cdot (\rho \mathbf{V}) \; = \; 0. \tag{2.10}$$

For constant density, above equation reduces into

$$\nabla \cdot \mathbf{V} = 0. \tag{2.11}$$

For two-dimensional incompressible flow continuity equation has form

$$\left(\frac{\partial}{\partial x}\hat{i} + \frac{\partial}{\partial y}\hat{j} \right) \cdot (u\hat{i} + v\hat{j}) = 0;$$

$$\nabla \cdot \mathbf{V} \; = \; \left(\frac{\partial u}{\partial x} + \frac{\partial v}{\partial y} \right) \; = \; 0. \tag{2.12}$$

2.6.2   Momentum Equation

For fluid particles, the equation of generalized linear momentum is observed from the Newton's second law of motion. It is stated as "The net force F is equal to the rate of change of linear momentum with time" . Newton's second law can be written as

$$m\frac{D\mathbf{V}}{Dt} = F; \tag{2.13}$$

9

The differential equation for this flow of the fluid is known as Navier-Strokes equation and has the form

$$\rho\frac{D\mathbf{V}}{Dt} = \nabla \cdot \tau + \rho\mathbf{b}; \qquad (2.14)$$

where $\rho\mathbf{b}$ denotes net body force, $\nabla \cdot \tau_*$ denotes surface forces and τ_* denotes Cauchy stress tensor.

For Navier-Stokes equation

$$\tau_* = -pI + \mu A;$$

where,

$$A_1 = (gradV) + (gradV)^T$$

In the above equations, $\frac{D}{Dt}$ denotes the total derivative, V denotes velocity field, ρ denotes density, b the body forces, p is the pressure and μ the dynamic viscosity. The stress tensor τ is expressed in the matrix form as

$$\tau = \begin{bmatrix} \sigma_{xx} & \tau_{yx} & \tau_{zx} \\ \tau_{xy} & \sigma_{yy} & \tau_{zy} \\ \tau_{xz} & \tau_{yz} & \sigma_{zz} \end{bmatrix}$$

where σxx, σyy and σzz are normal stresses. For two-dimensional flow, we have $V = [u(x,y,0); v(x,y,0); 0]$ and thus

$$grad\, V = \begin{bmatrix} \frac{\partial u}{\partial x} & \frac{\partial u}{\partial y} & 0 \\ \frac{\partial v}{\partial x} & \frac{\partial v}{\partial y} & 0 \\ 0 & 0 & 0 \end{bmatrix}$$

$$\frac{\partial u}{\partial t} + u\frac{\partial u}{\partial x} + v\frac{\partial u}{\partial y} = -\frac{1}{\rho}\frac{\partial p}{\partial x} + \nu\left[\frac{\partial^2 u}{\partial x^2} + \frac{\partial^2 u}{\partial y^2}\right]$$

10

Similarly, we repeat the above process for Y component as follows:

$$\frac{\partial v}{\partial t} + u\frac{\partial v}{\partial x} + v\frac{\partial v}{\partial y} = -\frac{1}{\rho}\frac{\partial p}{\partial y} + \nu\left[\frac{\partial^2 v}{\partial x^2} + \frac{\partial^2 v}{\partial y^2}\right].$$

Derivation of momentum equation for unsteady, non-Newtonian Maxwell nanofluid flow is given by

$$\rho a = \nabla \cdot \tau_*, \tag{2.15}$$

where $\tau_* = -pI + S$, where p is pressure and S is extra stress tensor of Maxwell fluid which satisfies the relation

$$\rho a = \nabla(-pI + \mu A), \tag{2.16}$$

$$\rho a = -\nabla pI + \nabla \cdot \mu A, \tag{2.17}$$

and $S + \lambda\frac{DS}{Dt} = \mu A$ satisfies the relation,

$$\rho\left[a + \lambda\frac{Da}{Dt}\right] = \nabla \cdot (\mu A), \tag{2.18}$$

$$\rho\left[a + \lambda\frac{Da}{Dt}\right] = \mu\nabla \cdot A, \tag{2.19}$$

For the velocity flow of the form $\vec{v} = [v_1(x, y), v_2(x, y)]$ and $A = (\nabla.V) + (\nabla.V)^T$,

$$A = \begin{bmatrix} 2\frac{\partial v_1}{\partial x} & \frac{\partial v_1}{\partial y} + \frac{\partial v_2}{\partial y} \\ \frac{\partial v_1}{\partial y} + \frac{\partial v_2}{\partial x} & 2\frac{\partial v_2}{\partial y} \end{bmatrix} \tag{2.20}$$

$$(\nabla \cdot A)_x = 2\frac{\partial^2 v_1}{\partial x^2} + \frac{\partial^2 v_1}{\partial y^2} + \frac{\partial^2 v_2}{\partial x\partial y}, \tag{2.21}$$

11

$$(\nabla \cdot A)_y = \frac{\partial^2 v_2}{\partial x^2} + 2\frac{\partial^2 v_2}{\partial y^2} + \frac{\partial^2 v_1}{\partial x \partial y}. \tag{2.22}$$

$$\left[\frac{Da_x}{Dt}\right] = (v_1)^2\frac{\partial^2 v_1}{\partial x^2} + 2v_1 v_2\frac{\partial^2 v_1}{\partial y \partial x} + (v_2)^2\frac{\partial^2 v_1}{\partial y^2} - v_1\left(\frac{\partial v_1}{\partial x}\right)^2 - v_2\frac{\partial v_1}{\partial x}\frac{\partial v_1}{\partial y} - v_1\frac{\partial v_2}{\partial x}\frac{\partial v_1}{\partial y} - v_2\left(\frac{\partial v_2}{\partial y}\right)^2, \tag{2.23}$$

$$\left[\frac{Da_y}{Dt}\right] = (v_1)^2\frac{\partial^2 v_2}{\partial x^2} + 2v_1 v_2\frac{\partial^2 v_2}{\partial y \partial x} + v^2\frac{\partial^2 v_2}{\partial y^2} - u\frac{\partial v_1}{\partial x}\frac{\partial v_2}{\partial x} - v_2\frac{\partial v_1}{\partial y}\frac{\partial v_2}{\partial x} - v_1\frac{\partial v_2}{\partial x}\frac{\partial v}{\partial y} - v_2\left(\frac{\partial v_2}{\partial y}\right)^2, \tag{2.24}$$

Boundary layer approximation yields,

$$\frac{\partial v_1}{\partial t} + v_1\frac{\partial v_1}{\partial x} + v_2\frac{\partial v_1}{\partial y} + \lambda\left[(v_1)^2\frac{\partial^2 v_1}{\partial x^2} + (v_2)^2\frac{\partial^2 v_1}{\partial y^2} + 2v_1 v_2\frac{\partial^2 v_1}{\partial y \partial x}\right] = \frac{\mu}{\rho}\left[\frac{\partial^2 v_1}{\partial y^2}\right], \tag{2.25}$$

$$\frac{\partial v_2}{\partial t} + v_1\frac{\partial v_2}{\partial x} + v_2\frac{\partial v_2}{\partial y} + \lambda\left[(v_1)^2\frac{\partial^2 v_2}{\partial x^2} + (v_2)^2\frac{\partial^2 v_2}{\partial y^2} + 2v_1 v_2\frac{\partial^2 v_2}{\partial y \partial x}\right] = \frac{\mu}{\rho}\left[\frac{\partial^2 v_2}{\partial y^2}\right]. \tag{2.26}$$

2.6.3 Energy Equation

According to the law of conservation of energy, total energy involved in a given closed system remains unchanged except the change of form. The equation of energy conservation can be composed as

$$\rho C_p \frac{D\mathbf{T}}{Dt} = \nabla \cdot (k\nabla T) + f \cdot \mathbf{V}. \tag{2.27}$$

In the above expression, C_p is specific heat capacity, κ is thermal conductivity and f is surface or body force.

2.7 Heat transfer

It is a process in which thermal energy transfers due to temperature differences between the physical systems. Different ways of heat transfer are discussed under.

2.7.1 Conduction

The flow of heat through a solid or liquid by the intersection of free electrons and molecules is said to be conduction. In other words, the heat transfer from one body to another due to the molecular agitation with a material without any motion of the material as whole is called conduction. Mathematical form of the law is

$$q = -kA\frac{\triangle T}{\triangle n},\qquad(2.28)$$

where q represents heat flow rate, A is cross-sectional area, k and $\frac{\triangle T}{\triangle n}$ denotes the constant of thermal conductivity and gradient of temperature respectively.

2.7.2 Convection

It is defined as heat transfer in fluids from a part with high temperature to a part where temperature is comparatively low.

2.7.3 Radiation

The emission of energy in the form of waves or particles is known as radiation. For example, if we place a material object (e.g, a piece of steel) under the sun rays, after a few moments, we observe that the material object is heated. Such phenomenon

takes place due to radiation. Mathematically, it can be formulated as

$$Q = \sigma \cdot T^4, \tag{2.29}$$

where σ, T and Q are the constant of Stephan-Boltzmann ($5.670 \times 10^{-8} \frac{W}{m^2 K^4}$), the temperature and the amount of heat transfered respectively.

2.8 Thermal diffusivity

Thermal diffusivity is a material property for unsteady heat conduction. Thermal diffusivity can be defined as the ratio of thermal conductivity to the density and specific heat capacity at constant pressure. It tells us that how much potential the material has for conducting thermal energy as compared to store it. Thermal diffusivity is usually denoted by α and expressed as

$$\alpha = \frac{\kappa}{\rho C_p}, \tag{2.30}$$

where C_p is the specific heat capacity, κ is thermal conductivity of material and ρ is the density.

2.9 Viscous dissipation

The process in which the work done by fluid is converted into heat is called viscous dissipation.

2.10   Boundary conditions

Boundary conditions are constraints which are necessary for boundary value problem and these must be satisfied at all or in a region in which system of differential equations has to be solved.

2.11   Boundary layer

The idea of boundary layer was first introduced by Ludwig Prandtl . Ludwig Prandtl gave the basic idea of the boundary layer for moving fluid over a surface [18]. It is the close layer of fluid flow near solid region where the viscosity effects are significant. The flow in this layer is usually laminar. The boundary layer thickness is the measure of the distance apart from the surface.

2.12   Nanofluids

A special class of liquids containing nanometer-size particles is the material which alters contained particles is called nanofluid. Nanofluid, is a term used to describe special class of fluids in which nanometer-sized particles are dispersed in water and base fluids.

2.13   Physical properties of nanofluid

Some of the physical parameters used in the discussion of nanofluids are mentioned below.

2.13.1 Viscosity

Nanofluids viscosity defined by Brinkman [19] is given as

$$\mu_{nf} = \frac{\mu_f}{(1-\Phi)^{2.5}}. \tag{2.31}$$

In the above equation, ϕ gives nanoparticle volume fraction coefficient while μ_f denotes dynamic viscosity of base fluid.

2.13.2 Density

Khanafer et al. [20] expressed the density of nanofluid as

$$\rho_{nf} = (1-\Phi)\rho_f + \Phi\rho_s, \tag{2.32}$$

where ρ_f and ρ_s represents the density of base fluid and solid nanoparticles respectively.

2.13.3 Specific heat

Specific heat of nanofluid has the relation given as

$$(\rho C_p)_{nf} = (1-\Phi)(\rho C_p)_f + \Phi(\rho C_p)_s, \tag{2.33}$$

where $(C_p)_s$ denotes specific heat of the solid nanoparticle and $(C_p)_f$ denotes specific heat capacity of base fluid.

2.13.4   Thermal conductivity

It is given by Maxwell as

$$k_{nf} = k_f \left[\frac{k_s + 2k_f - 2\Phi(k_f - k_s)}{k_s + 2k_f + \Phi(k_f - k_s)} \right], \tag{2.34}$$

where k_s and k_f denotes thermal conductivity of both nanoparticle and base fluid.

2.14   Entropy of a system

Entropy is a function of a quantity of heat which shows the possibility of conversion of that heat into work. Entropy is a thermodynamic property; it can be viewed as a measure of disorder.

2.15   Dimensionless numbers

2.15.1   Skin friction coefficient

Skin friction coefficient represents the value of friction which occurs when fluid moves across the surface. The skin friction coefficient Abel *et al.* [21] can be defined as

$$C_f = \frac{\tau_w}{\rho U_w{}^2}. \tag{2.35}$$

2.15.2 Nusselt number Nu

It is defined as the ratio between transfer of heat by convection (h) and heat transport by conduction (k) in the direction normal to the boundary.

$$Nu = \frac{hL}{k}, \qquad (2.36)$$

L stands for characteristics length. In this thesis, we are taking Nu as

$$Nu_x = \frac{xq_w}{k_f(T_w - T_\infty)}, \qquad (2.37)$$

with wall heat flux q_w as $q_w = -k_{nf}\left(1 + \frac{16\sigma^* T_\infty^3}{3k^* k_f}\right)\left(\frac{\partial T}{\partial y}\right)_{y=0}$

2.15.3 Eckert number Ec

Eckert number relates the kinetic energy to the enthalpy (∇T) of fluid and it is used to characterized the effect of self heating of a fluid as an outcome of heat dissipation. It is mathematically expressed as

$$Ec = \frac{U_w^2}{C_p(T_w - T_\infty)}. \qquad (2.38)$$

where C_p is specific heat capacity U_w denotes the free stream velocity, T_w is wall temperature and T_∞ is temperature far away from wall.

18

2.15.4 Prandtl number Pr

It gives the quantitative relation between the momentum diffusion ν rate and thermal diffusion α rate.

$$P_r = \frac{\text{momentum diffusivity}}{\text{thermal diffusivity}} = \frac{\nu_f}{\alpha_f} \tag{2.39}$$

where $\alpha_f = \frac{\kappa_f}{(\rho C_p)_f}$ is the thermal diffusivity parameter. The relative thickness of thermal and momentum boundary layer is controlled by Prandtal number. For small P_r, heat distributed rapidly corresponds to the momentum.

2.16 Similarity transformation

Similarity transformation is a tool used in mathematics, which helps in transformation of partial differential equations, which occurs in a problem, into ordinary differential equations. Similarity transformation reduces the number of independent variables of partial differential equation. It can be stated in a way that it is a rule which combines the two independent variable to get a new one.

2.17 Keller Box Method

Keller-box method was first reported by Keller in 1970. Which has become popular for obtaining approximate solutions for boundary layer problems. This method has second order convergence. Keller box method has been extensively applied on laminar boundary layer flows. This method results more efficiently then other methods. We first write the governing differential equations into a first order system.

After reduction of odes to first order system, domain is discretized which allows to calculate the approximate solution over each sub domain rather then over entire domain. To get finite difference equations with a second order truncation error, simple backward-difference derivatives and average of the midpoints of net rectangles are used. The resulting algebraic equations are then linearized by using Newton's method as Keller [22] elaborated. And, write them in matrix-vector form. A block tridiagonal matrix is basically a tridiagonal matrix but has sub matrices in places of scalars. It has super diagonal, diagonal and sub diagonal square matrices (blocks) in place of upper, main and lower diagonal entries respectively. And all other blocks are zero matrices. Finally LU decomposition is used to obtain the final result.

Chapter 3

Thermal and Entropy Analysis of Maxwell Nanofluid with Slip Conditions, Thermal Radiations and Variable Thermal Conductivity

This chapter provides a detailed review of work presented by A. Aziz *et al.* [13]. The mathematical model study the flow and heat transfer characteristics of Maxwell nanofluid over a non-uniform porous stretching surface in a uniform porous medium. The problem is considered with partial slip and convective conditions at the surface. Thermal radiation, MHD and variable thermal conductivity are also taken into account. The governing pdes are first modeled and then reduced into a set of odes by using suitable similarity transformations. The resulting odes are then solved numerically by Keller box method. The features and characteristics of fluid flow are discussed for different values of governing flow parameters. The numerical

computations are also performed to calculate the skin friction coefficient and the local Nusselt number. The results are computed for Copper water and Titanium water nanofluids.

The governing partial differential equations are presented in Section 3.1. Similarity transformations and reduction of governing pdes to system of non-linear odes are given in Section 3.2. Section 3.3 provided details of Keller box method and the numerical computations, finally Section 3.4 comprises the discussion of numerical results.

3.1 Mathematical model

Let us assume an incompressible non-Newtonian Maxwell nanofluid with heat transfer characteristics. The two-dimensional unsteady and laminar flow is considered over the porous stretching sheet of non-uniform velocity $U_w(x,t) = \frac{ax}{1-\xi t}$ where a is an initial stretching rate with dimension $[T^{-1}]$ and $\xi < \frac{1}{t}$. Insulated sheet temperature is $T_w(x,t) = T_\infty + \frac{ax}{1-\xi t}$ and for convenience it is assumed to be fixed at x=0, where T_w and T_∞ represent the temperature of wall and surroundings respectively. Partial slip and convective conditions are also considered at the boundary. Uniform magnetic field is applied in normal direction to the flow and strength of magnetic field is given by $B(t) = \frac{B_0}{\sqrt{1-\xi t}}$.

The continuity, momentum, energy and entropy equations described in [17] modified for the unsteady two-dimensional Maxwell nanofluid flow under usual boundary layer approximations along with thermal radiation and variable thermal conductivity are

$$\frac{\partial v_1}{\partial x} + \frac{\partial v_2}{\partial y} = 0, \tag{3.1}$$

22

$$\frac{\partial v_1}{\partial t} + v_1 \frac{\partial v_1}{\partial x} + v_2 \frac{\partial v_1}{\partial y} = \frac{\mu_{nf}}{\rho_{nf}} \frac{\partial^2 v_1}{\partial y^2} - \lambda \left[v_1^2 \frac{\partial^2 v_1}{\partial x^2} + v_2^2 \frac{\partial^2 v_1}{\partial y^2} + 2v_1 v_2 \frac{\partial^2 v_1}{\partial x \partial y} \right] - \frac{\sigma_{nf} B^2(t) v_1}{\rho_{nf}} - \frac{\mu_{nf} v_1}{\rho_{nf} k},$$
$$(3.2)$$

$$\frac{\partial T}{\partial t} + v_1 \frac{\partial T}{\partial x} + v_2 \frac{\partial T}{\partial y} = \frac{1}{(\rho C_p)_{nf}} \left[\frac{\partial}{\partial y} (\kappa_{nf}^\star(T)) \frac{\partial T}{\partial y} \right] - \frac{1}{(\rho C_p)_{nf}} \left(\frac{\partial q_r}{\partial y} \right), \qquad (3.3)$$

$$E_G = \frac{k_{nf}}{T_\infty^2} \left\{ \left(\frac{\partial T}{\partial y} \right)^2 + \frac{16\sigma^* T_\infty^3}{3k^*} \left(\frac{\partial T}{\partial y} \right)^2 \right\} + \frac{\mu_{nf}}{T_\infty} \left(\frac{\partial v_1}{\partial y} \right)^2 + \frac{\sigma_{nf} B^2(t) v_1^2}{T_\infty} + \frac{\mu_{nf} v_1^2}{T_\infty k}.$$
$$(3.4)$$

The following boundary conditions are assumed

$$v_1(x, 0, t) = U_w + W_1 \mu_{nf} \left(\frac{\partial v_1}{\partial y} \right), \quad v_2(x, 0, t) = V_w, \quad -\kappa \left(\frac{\partial T}{\partial y} \right) = h_f(T_w - T), \quad (3.5)$$

$$v_1 \longrightarrow 0, \quad T \longrightarrow T_\infty \ \ as \ \ y \longrightarrow \infty. \qquad (3.6)$$

Here the velocity of the flow is of the form $\vec{v} = [v_1(x, y, t), v_2(x, y, t), 0]$. Time is represented by t, T is a temperature of the fluid and k denotes porosity factor. Elasticity stress parameter is given by $\lambda = \lambda_0(1 - \xi t)$ with λ_0 a constant. The porosity of the stretching surface is represented by V_w and the velocity slip factor is given by $W_1 = W_0\sqrt{1 - \xi t}$ with an initial slip value (W_0). $\kappa_{nf}^*(T) = k_{nf} \left[1 + \epsilon \frac{T - T_\infty}{T_w - T_\infty} \right]$ is the variable thermal conductivity.

In non-Newtonian Maxwell nanofluid radiation only travel a short distance due to thickness of fluid. Due to this phenomenon, Rosseland approximation for radiation [23] is used in equation (3.3) and it is given $\frac{\partial q_r}{\partial y} = -\frac{16T_\infty^3 \sigma^*}{3k^*} \frac{\partial^2 T}{\partial y^2}$. The dimensionless entropy generation (N_G) is given by $N_G = \frac{T_\infty^2 a^2 E_G}{\kappa_f (T_w - T_\infty)^2}$ (See Das *et al.* [24]).

3.2 Similarity Transformation

To solve the boundary value problem (BVP) (3.1) - (3.6) similarity technique is used to transform governing partial differential equations into ordinary differential equations. Introducing stream functions ψ of the form

$$v_1 = \frac{\partial \psi}{\partial y}, \quad v_2 = -\frac{\partial \psi}{\partial x}, \tag{3.7}$$

and similarity variables as

$$\chi(x, y, t) = \sqrt{\frac{a}{v_f(1 - \xi t)}})y, \quad \psi(x, y, t) = \sqrt{\frac{v_f a}{(1 - \xi t)}}xg(\chi), \quad \gamma(\chi) = \frac{T - T_\infty}{T_w - T_\infty}, \tag{3.8}$$

Calculating derivatives in order to determine the equations for the similarity solution of the problem.

Letting,

$$v_1 = \frac{\partial \psi}{\partial y}, \tag{3.9}$$

$$v_1 = \frac{\partial \psi}{\partial \chi} \cdot \frac{\partial \chi}{\partial y}, \tag{3.10}$$

$$\chi(x, y, t) = \sqrt{\frac{a}{\nu_f(1 - \xi t)}}y, \tag{3.11}$$

Differentiating w. r. t. 'y',

$$\frac{\partial \chi}{\partial y} = \sqrt{\frac{a}{\nu_f(1 - \xi t)}}, \tag{3.12}$$

$$\psi(x, y, t) = \sqrt{\frac{\nu_f a}{(1 - \xi t)}}xf(\chi), \tag{3.13}$$

$$\frac{\partial \psi}{\partial y} = \sqrt{\frac{\nu_f a}{(1 - \xi t)}}xg'(\chi)\left(\frac{\partial \chi}{\partial y}\right), \tag{3.14}$$

24

$$\frac{\partial \psi}{\partial y} = \frac{ax}{(1 - \xi t)} g'(\chi), \tag{3.15}$$

which gives,

$$v_1 = \frac{ax}{(1 - \xi t)} g'(\chi). \tag{3.16}$$

Now, we aim to find,

$$\frac{\partial v_1}{\partial x} = \frac{a}{(1 - \xi t)} g'(\chi). \tag{3.17}$$

Calculating v_2,

$$v_2 = -\frac{\partial \psi}{\partial x}, \tag{3.18}$$

Differentiating w. r. t. 'x',

$$\frac{\partial \psi}{\partial x} = \sqrt{\frac{\nu_f a}{(1 - \xi t)}} g(\chi), \tag{3.19}$$

we get expression for v_2,

$$v_2 = -\sqrt{\frac{\nu_f a}{(1 - \xi t)}} f(\chi). \tag{3.20}$$

$$\frac{\partial v_2}{\partial y} = -\sqrt{\frac{\nu_f a}{(1 - \xi t)}} g'(\chi) \left(\frac{\partial \chi}{\partial y} \right), \tag{3.21}$$

$$\frac{\partial v_2}{\partial y} = -\frac{a}{(1 - \xi t)} f'(\chi), \tag{3.22}$$

$$\frac{\partial v_1}{\partial x} + \frac{\partial v_2}{\partial y} = \frac{a}{(1 - \xi t)} g'(\chi) - \frac{a}{(1 - \xi t)} g'(\chi) = 0. \tag{3.23}$$

$$\frac{\partial v_1}{\partial t} = \frac{\partial}{\partial t} \left(\frac{ax}{(1 - \xi t)} g'(\chi) \right), \tag{3.24}$$

$$\frac{\partial v_1}{\partial t} = \frac{ax}{(1 - \xi t)^2} \left[\xi g' + \frac{\xi g''}{2} \right], \tag{3.25}$$

25

$$\frac{\partial v_1}{\partial x} = \frac{a}{(1 - \xi t)} g'(\chi), \tag{3.26}$$

$$v_1 \frac{\partial v_1}{\partial x} = \frac{ax}{(1 - \xi t)} g'(\chi) \left(\frac{a}{(1 - \xi t)} g'(\chi) \right), \tag{3.27}$$

$$v_1 \frac{\partial v_1}{\partial x} = \frac{a^2 x}{(1 - \xi t)^2} g'^2(\chi), \tag{3.28}$$

$$\frac{\partial v_1}{\partial y} = \frac{axg''(\chi)}{(1 - \xi t)} \sqrt{\frac{a}{\nu_f(1 - \xi t)}}, \tag{3.29}$$

$$v_2 \frac{\partial v_1}{\partial y} = -\sqrt{\frac{\nu_f a}{(1 - \xi t)}} g(\chi) \left(axg''(\chi) \sqrt{\frac{a}{\nu_f(1 - \xi t)}} y \right), \tag{3.30}$$

$$v_2 \frac{\partial v_1}{\partial y} = -\frac{a^2 x g(\chi) g''(\chi)}{(1 - \xi t)^2}. \tag{3.31}$$

$$\frac{\partial v_1}{\partial t} + v_1 \frac{\partial v_1}{\partial x} + v_2 \frac{\partial v_1}{\partial y} = \frac{a^2 x g}{(1 - \xi t)^2} \left[A(g' + \frac{\chi}{2} g'' + g'^2 - gg'') \right]. \tag{3.32}$$

where $A = \frac{\xi}{a}$. Now, solving the following term from equation (3.2).

$$= \lambda \left[(v_1)^2 \frac{\partial^2 v_1}{\partial x^2} + (v_2)^2 \frac{\partial^2 v_1}{\partial y^2} + 2 v_1 v_2 \frac{\partial^2 v_1}{\partial x \partial y} \right], \tag{3.33}$$

Calculating derivatives in sequence,

$$\frac{\partial^2 v_1}{\partial y^2} = \frac{\partial}{\partial y} \left(\frac{axg''(\chi)}{(1 - \xi t)} \sqrt{\frac{a}{\nu_f(1 - \xi t)}} \right), \tag{3.34}$$

$$\frac{\partial^2 v_1}{\partial y^2} = \left(\frac{axg'''(\chi)}{(1 - \xi t)} \sqrt{\frac{a}{\nu_f(1 - \xi t)}} \right) \frac{\partial \chi}{\partial y}, \tag{3.35}$$

$$\frac{\partial^2 v_1}{\partial y^2} = \left(\frac{a^2 x g'''(\chi)}{(1 - \xi t)^2 \nu_f} \right), \tag{3.36}$$

26

$$\frac{\partial^2 v_1}{\partial x^2} = 0, \tag{3.37}$$

$$\frac{\partial^2 v_1}{\partial x \partial y} = \left(\frac{ag''(\chi)}{(1 - \xi t)} \sqrt{\frac{a}{\nu_f (1 - \xi t)}} \right) \tag{3.38}$$

$$2v_1 v_2 = 2 \left(\frac{ax}{(1 - \xi t)} g'(\chi) \right) \left(-\sqrt{\frac{\nu_f a}{(1 - \xi t)}} g(\chi) \right), \tag{3.39}$$

$$2v_1 v_2 \left(\frac{\partial^2 v_1}{\partial x \partial y} \right) = \frac{-2a^3 g g' g'' x}{(1 - \xi t)^3}, \tag{3.40}$$

$$(v_1)^2 = \frac{a^2 x^2 g'^2(\chi)}{(1 - \xi t)^2}, \tag{3.41}$$

$$(v_1)^2 \left(\frac{\partial^2 v_1}{\partial x^2} \right) = 0, \tag{3.42}$$

$$(v_2)^2 = \frac{\nu_f a g^2(\chi)}{(1 - \xi t)}, \tag{3.43}$$

$$(v_2)^2 \frac{\partial^2 v_1}{\partial y^2} = \frac{x a^3 g^2(\chi) g'''(\chi)}{(1 - \xi t)^3}, \tag{3.44}$$

$$\lambda \left[(v_1)^2 \frac{\partial^2 (v_1)}{\partial x^2} + (v_1)^2 \frac{\partial^2 v_1}{\partial y^2} + 2v_1 v_2 \frac{\partial^2 v_1}{\partial x \partial y} \right] = \lambda \left[0 + \frac{x a^3 g^2(\chi) g'''(\chi)}{(1 - \xi t)^3} - \frac{2a^3 g g' g'' x}{(1 - \xi t)^3} \right], \tag{3.45}$$

$$\lambda \left[(v_1)^2 \frac{\partial^2 v_1}{\partial x^2} + (v_2)^2 \frac{\partial^2 v_1}{\partial y^2} + 2v_1 v_2 \frac{\partial^2 v_1}{\partial x \partial y} \right] = -\frac{\lambda_o a^3 x}{(1 - \xi t)^2} \left(g^2 g''' - 2g g' g'' \right). \tag{3.46}$$

Now solving remaining terms of equation (3.2)

$$= \frac{\mu_{nf}}{\rho_{nf}} \left(\frac{\partial^2 v_1}{\partial y^2} \right) - \frac{\sigma_{nf} B^2(t) v_1}{\rho_{nf}} - \frac{\mu_{nf}}{\rho_{nf} k} v_1, \tag{3.47}$$

$$= \frac{\mu_{nf}}{\rho_{nf}} \left(\left(\frac{a^2 x g'''(\chi)}{(1 - \xi t)^2 \nu_f} \right) \right) - \frac{\sigma_{nf} B^2(t)}{\rho_{nf}} \left(\frac{ax}{(1 - \xi t)} g'(\chi) \right) - \frac{\mu_{nf}}{\rho_{nf} k} \left(\frac{ax}{(1 - \xi t)} g'(\chi) \right), \tag{3.48}$$

$$= \frac{a^2 x}{(1 - \xi t)^2} \left[\frac{\mu_f g'''}{\rho_f \Phi_1 \Phi_2 \nu_f} - \frac{\sigma_f \Phi_4 B_o^2 g'}{\rho_f \Phi_2} a - \frac{\mu_f g'(1 - \xi t)}{\rho_f \Phi_1 \Phi_2 a k} \right], \tag{3.49}$$

27

$$\frac{\mu_{nf}}{\rho_{nf}}\left(\frac{\partial^2 u}{\partial y^2}\right) - \frac{\sigma_{nf}B^2(t)u}{\rho_{nf}} - \frac{\mu_{nf}}{\rho_{nf}k}u = \frac{a^2 x}{(1-\xi t)^2}\left[\frac{g'''}{\Phi_1\Phi_2} - \frac{\Phi_4}{\Phi_2}Mf' - \frac{Kg'}{\Phi_1\Phi_2}\right], \quad (3.50)$$

Inserting (3.32), (3.46) and (3.50) in (3.2), yields the ODE

$$A\left(\frac{\chi}{2}g'' + g'\right) + g'^2 - gg'' - \frac{g'''}{\Phi_1\Phi_2} + \beta\left(g^2 g''' - 2gg'g''\right) + \frac{\Phi_4}{\Phi_2}Mg' + \frac{1}{\Phi_1\Phi_2}Kg' = 0. \quad (3.51)$$

Using the next transformation,

$$\gamma(\chi) = \frac{T - T_\infty}{T_w - T_\infty} \quad (3.52)$$

$$T_w - T_\infty = \frac{ax}{(1-\xi t)} \quad (3.53)$$

$$\gamma(\chi)\frac{ax}{(1-\xi t)} = (T - T_\infty) \quad (3.54)$$

$$T = T_\infty + \frac{ax}{(1-\xi t)}\gamma(\chi) \quad (3.55)$$

Differentiating above expression w. r. t. 'x', 'y' and 't',

$$\frac{\partial T}{\partial x} = \frac{a}{(1-\xi t)}\gamma(\chi), \quad (3.56)$$

$$v_1\left(\frac{\partial T}{\partial x}\right) = \left(\frac{ax}{(1-\xi t)}g'(\chi)\right)\frac{a}{(1-\xi t)}\gamma(\chi), \quad (3.57)$$

$$\frac{\partial T}{\partial y} = \frac{ax}{(1-\xi t)}\gamma'(\chi)\left(\frac{\partial \chi}{\partial y}\right) \quad (3.58)$$

28

$$\frac{\partial T}{\partial y} = \frac{ax}{(1-\xi t)}\gamma'(\chi)\sqrt{\frac{a}{\nu_f(1-\xi t)}}, \tag{3.59}$$

$$v_2\left(\frac{\partial T}{\partial y}\right) = \left(-\sqrt{\frac{\nu_f a}{(1-\xi t)}}g(\chi)\right)\frac{ax}{(1-\xi t)}\gamma'(\chi)\sqrt{\frac{a}{\nu_f(1-\xi t)}} \tag{3.60}$$

$$\frac{\partial T}{\partial t} = \frac{\xi ax}{(1-\xi t)^2} + \frac{ax}{(1-\xi t)}\gamma'(\chi)\left(\frac{\partial \chi}{\partial t}\right) \tag{3.61}$$

$$\frac{\partial T}{\partial t} = \frac{\xi ax}{(1-\xi t)^2} + \frac{ax}{(1-\xi t)}\gamma'(\chi)\left(\sqrt{\frac{1}{\nu_f(1-\xi t)}}y\left(\frac{\xi}{1-\xi t}\frac{1}{2}\right)\right) \tag{3.62}$$

$$\frac{\partial T}{\partial t} = \frac{\xi ax}{(1-\xi t)^2} + \frac{\xi ax}{2(1-\xi t)^2}\gamma'(\chi), \tag{3.63}$$

$$\frac{\partial T}{\partial t} = \frac{\xi ax}{(1-\xi t)^2}\left(\gamma(\chi) + \frac{\chi}{2}\gamma'(\chi)\right), \tag{3.64}$$

$$\frac{\partial T}{\partial t} = \frac{\xi a^2 x}{a(1-\xi t)^2}\left(\gamma(\chi) + \frac{\chi}{2}\gamma'(\chi)\right), \tag{3.65}$$

$$\frac{\partial T}{\partial t} = \frac{a^2 x}{(1-\xi t)^2}A\left(\gamma(\chi) + \frac{\chi}{2}\gamma'(\chi)\right), \tag{3.66}$$

$$\frac{\partial T}{\partial t} + v_1\frac{\partial T}{\partial x} + v_2\frac{\partial T}{\partial y} = \frac{a^2 x}{(1-\xi t)^2}A\left(\gamma(\chi) + \frac{\chi}{2}\gamma'(\chi)\right) + \left(\frac{ax}{(1-\xi t)}g'(\chi)\right)\frac{a}{(1-\xi t)}\gamma(\chi)$$
$$- \left(\sqrt{\frac{\nu_f a}{(1-\xi t)}}g(\chi)\right)\frac{ax}{(1-\xi t)}\gamma'(\chi)\sqrt{\frac{a}{\nu_f(1-\xi t)}}. \tag{3.67}$$

Left hand side of equation (3.3) is given by,

$$\frac{\partial T}{\partial t} + v_1 \frac{\partial T}{\partial x} + v_2 \frac{\partial T}{\partial y} = \frac{a^2 x}{(1 - \xi t)^2} \left[A(\gamma + \frac{\chi}{2}\gamma') + \gamma g' - \gamma' g \right]. \qquad (3.68)$$

Now, solving the other side of equation (3.3)

$$= \frac{1}{(\rho C_p)_{nf}} \left[\frac{\partial}{\partial y} \left(k_{nf} \left[1 + \epsilon \frac{T - T_\infty}{T_w - T_\infty} \right] \left(\frac{ax}{(1 - \xi t)} \gamma'(\chi) \sqrt{\frac{a}{\nu_f(1 - \xi t)}} \right) \right) \right], \qquad (3.69)$$

$$= \frac{1}{(\rho C_p)_{nf}} \left[\frac{\partial}{\partial y} \left(k_{nf} \left[1 + \epsilon \gamma \right] \left(\frac{ax}{(1 - \xi t)} \gamma'(\chi) \sqrt{\frac{a}{\nu_f(1 - \xi t)}} \right) \right) \right], \qquad (3.70)$$

$$\frac{1}{(\rho C_p)_{nf}} \left[\frac{\partial}{\partial y}(\kappa_{nf}^*(T) \frac{\partial T}{\partial y}) \right] = \frac{k_{nf}}{(\rho C_p)_{nf}} \left[\left(\frac{ax}{(1 - \xi t)} \sqrt{\frac{a}{\nu_f(1 - \xi t)}} \right) \frac{\partial}{\partial y}(1 + \epsilon\gamma(\chi))\gamma' \right], \qquad (3.71)$$

$$\frac{1}{(\rho C_p)_{nf}} \left[\frac{\partial}{\partial y}(\kappa_{nf}^*(T) \frac{\partial T}{\partial y}) \right] = \frac{k_{nf}}{(\rho C_p)_{nf}} \frac{a^2 x}{(1 - \xi t^2)} \left[\epsilon\gamma^2 + (1 + \epsilon\gamma)\gamma'' \right], \qquad (3.72)$$

$$\frac{1}{(\rho C_p)_{nf}} \left[\frac{\partial}{\partial y}(\kappa_{nf}^*(T) \frac{\partial T}{\partial y}) \right] = \frac{\Phi_5 k_f}{\Phi_3 (\rho C_p)_f} \frac{a^2 x}{(1 - \xi t)^2} \left[\epsilon\gamma^2 + (1 + \epsilon\gamma)\gamma'' \right], \qquad (3.73)$$

$$\frac{1}{(\rho C_p)_{nf}} \left[\frac{\partial}{\partial y}(\kappa_{nf}^*(T) \frac{\partial T}{\partial y}) \right] = \frac{\Phi_5}{\Phi_3} \frac{\alpha_f}{\nu_f} \frac{a^2 x}{(1 - \xi t)^2} \left[\epsilon\gamma^2 + (1 + \epsilon\gamma)\gamma'' \right], \qquad (3.74)$$

30

$$\frac{1}{(\rho C_p)_{nf}} \left[\frac{\partial}{\partial y} \left(\kappa_{nf}^*(T) \frac{\partial T}{\partial y} \right) \right] = \frac{\Phi_5}{\Phi_3} \frac{1}{Pr} \frac{a^2 x}{(1-\xi t)^2} \left[\epsilon \gamma^2 + (1+\epsilon\gamma)\gamma'' \right], \qquad (3.75)$$

$$-\frac{1}{(\rho C_p)_{nf}} \left[\frac{\partial q_r}{\partial y} \right] = -\frac{1}{(\rho C_p)_{nf}} \frac{-16\sigma^* T^3}{3k^*} \left(\frac{\partial^2 T}{\partial y^2} \right), \qquad (3.76)$$

$$\left(\frac{\partial^2 T}{\partial y^2} \right) = \frac{a^2 x}{\nu_f (1-\xi t)^2}, \qquad (3.77)$$

$$\frac{1}{(\rho C_p)_{nf}} \left[\frac{\partial q_r}{\partial y} \right] = \frac{a^2 x}{\nu_f (1-\xi t)^2} \left[\frac{16\sigma^* T^3}{3k^* \nu_f \rho C_p)_f} \frac{\gamma''}{\Phi_3} \right], \qquad (3.78)$$

$$\frac{1}{(\rho C_p)_{nf}} \left[\frac{\partial q_r}{\partial y} \right] = \frac{a^2 x}{(1-\xi t)^2} \left[\frac{Nr\gamma''}{\Phi_3} \right]. \qquad (3.79)$$

$$\left[A(\gamma + \frac{\chi}{2}\gamma') + \gamma g' - \gamma' g \right] - \frac{\Phi_5}{\Phi_3} \frac{1}{Pr} \left[\epsilon\gamma^2 + (1+\epsilon\gamma)\gamma'' \right] - \left[\frac{Nr\gamma''}{\Phi_3} \right], \qquad (3.80)$$

Inserting (3.68), (3.75) and (3.79) in (3.3), yields the following ODE

$$\gamma'' \left(1 + \epsilon\gamma + \frac{1}{\Phi_5} PrNr \right) + \epsilon\gamma'^2 + Pr\frac{\Phi_3}{\Phi_5} \left[g\gamma' - g'\gamma - A(\gamma + \frac{\chi}{2}\gamma') \right] = 0. \qquad (3.81)$$

The transformed ODE of entropy is given as under

$$N_G = Re \left[\Phi_5(1+Nr)\gamma'^2 + \frac{Br}{\Phi_5\Omega} \left(g''^2 + \Phi_1\Phi_4 Mg'^2 + Kg'^2 \right) \right]. \qquad (3.82)$$

with

$$g(0) = S, \quad g'(0) = 1 + \frac{\Lambda}{\Phi_1} g''(0), \quad \gamma'(0) = -B_i(1 - \gamma(0)), \qquad (3.83)$$

$$g'(\chi) \longrightarrow 0, \quad \gamma(\chi) \longrightarrow 0 \quad as \quad \chi \longrightarrow \infty, \qquad (3.84)$$

31

where $\Phi'_i s, \quad 1 \leqslant i \leqslant 5$ in above equations represents the following thermo physical properties for the Maxwell nanoluid

$$\Phi_1 = (1 - \Phi)^{2.5}, \quad \Phi_2 = \left(1 - \Phi + \Phi\frac{\rho_s}{\rho_f}\right), \quad \Phi_3 = \left(1 - \Phi + \Phi\frac{(\rho C_p)_s}{(\rho C_p)_f}\right), \quad (3.85)$$

$$\Phi_4 = \left(1 + \frac{3(\frac{\sigma_s}{\sigma_f} - 1)\Phi}{(\frac{\sigma_s}{\sigma_f} + 2) - (\frac{\sigma_s}{\sigma_f} - 1)\Phi}\right), \quad \Phi_5 = \left(\frac{(k_s + 2k_f) - 2\Phi(k_f - k_s)}{(k_s + 2k_f) + \Phi(k_f - k_s)}\right). \quad (3.86)$$

Unsteadiness, Maxwell, magnetic and porous medium parameters are defined here by $A = \frac{\xi}{a}$, $\beta = a\lambda_0$, $M = \frac{\sigma_f B_o^2}{a\rho_f}$ and $K = \frac{\nu_f(1-\xi t)}{ak}$ respectively. $Pr = \frac{\nu_f}{\alpha_f}$ is the Prandtl number. Thermal diffusivity parameter, mass transfer parameter and thermal radiation parameter are given by $\alpha_f = \frac{\kappa_f}{(\rho C_p)_f}$, $S = -V_w\sqrt{\frac{1-\xi t}{\nu_f a}}$ and $Nr = \frac{16}{3}\frac{\sigma^* T_\infty^3}{\kappa^* \nu_f (\rho C_p)_f}$ respectively. $\Lambda = W_0\sqrt{\frac{a}{\nu_f}}\mu_f$ is the velocity slip parameter and $B_i = \frac{h_f}{k_f}\sqrt{\frac{\nu_f(1-\xi t)}{a}}$ is the Biot number. Re and Br in equation (3.82) represents Reynolds and Brinkmann number respectively. Dimensionless temperature gradient is given by $\Omega = \frac{T_w - T_\infty}{T_\infty}$.

After applying the non-dimensional transformations (3.7) on reduced skin friction (C_f) and Nusselt numbers (Nu_x) explained in Chapter [2], the following equations are obtained

$$C_f Re_x^{1/2} = -\frac{g''(0)}{(1 - \Phi)^{2.5}}, \quad Nu_x Re_x^{1/2} = \frac{\kappa_{nf}}{\kappa_f}(1 + Nr)\gamma'(0), \quad (3.87)$$

$Re_x = \frac{U_w x}{\nu_f}$ is the local Reynolds number which depends on initial stretching velocity U_w.

3.3 Finding Solution

Numerical solution of equations (3.51), (3.81) and (3.82) with subject to conditions (3.83) - (3.84) is found by implementation of Keller-box numerical scheme. In order to apply the Keller-box numerical scheme, it is necessary to write equations (3.51), (3.81) and (3.82) into a first-order system with some new introduced variables.

$$v_1 = g', \tag{3.88}$$

$$v_2 = v_1', \tag{3.89}$$

$$t = \gamma', \tag{3.90}$$

$$A\left(\frac{\chi}{2}v_2 + v_1\right) + v_1^2 - gv_2 - \frac{v_2'}{\Phi_1\Phi_2} + \beta(g^2v_2 - 2gv_1v_2) + \frac{\Phi_4}{\Phi_2}Mv_1 + \frac{1}{\Phi_1\Phi_2}\kappa v_1 = 0, \tag{3.91}$$

$$t'(1 + \epsilon\gamma + 1\Phi_5 PrNr) + \epsilon t^2 + Pr\frac{\Phi_3}{\Phi_5}[gt - v_1\gamma - A(\gamma + \frac{\chi}{2}t)] = 0, \tag{3.92}$$

$$N_G = Re\left[\Phi_5(1 + Nr)t^2 + \frac{Br}{\Phi_5\Omega}\left(v_1'^2 + \Phi_1\Phi_4 Mv_1^2 + Kv_1^2\right)\right] \tag{3.93}$$

and conditions are

$$g(0) = S, \quad v_1(0) = 1 + \frac{\Lambda}{\Phi_1}v_2(0), \quad t(0) = -B_i(1 - \gamma(0)), \tag{3.94}$$

$$v_1(\infty) \longrightarrow 0, \quad \gamma(\infty) \longrightarrow 0. \tag{3.95}$$

After obtaining first-order system, discritize the domain which allows to calculate the approximate solution over each sub domain rather then over entire domain.

$$\chi_0 = 0; \quad \chi_n = \chi_{n-1} + h, \quad n = 1, 2, 3, ..., N - 1; \quad \chi_N = \chi_\infty.$$

Then difference equations are obtained using backward differences. Functions are replaced with their mean averages. The system of ODEs (3.88)-(3.93) is then converted into the following algebraic equations.

$$\frac{(v_1)_n + (v_1)_{n-1}}{2} = \frac{g_n - g_{n-1}}{h}, \tag{3.96}$$

$$\frac{(v_2)_n + (v_2)_{n-1}}{2} = \frac{(v_1)_n - (v_1)_{n-1}}{h}, \tag{3.97}$$

$$\frac{t_n + t_{n-1}}{2} = \frac{\gamma_n - \gamma_{n-1}}{h}, \tag{3.98}$$

$$A\left\{\left(\frac{(v_1)_n + (v_1)_{n-1}}{2}\right) + \frac{\chi}{2}\right\} + \left(\frac{(v_1)_n + (v_1)_{n-1}}{2}\right)^2 -$$
$$\left(\frac{g_n + g_{n-1}}{2}\right)\left(\frac{(v_2)_n + (v_2)_{n-1}}{2}\right) - \frac{1}{\Phi_1 \Phi_2}\left(\frac{(v_2)_n - (v_2)_{n-1}}{h}\right) + \beta$$
$$\left(\left(\frac{g_n + g_{n-1}}{2}\right)^2\left(\frac{(v_2)_n - (v_2)_{n-1}}{h}\right) - 2\left(\frac{g_n + g_{n-1}}{2}\right)\left(\frac{(v_1)_n + (v_1)_{n-1}}{2}\right)\right)$$
$$\left(\frac{(v_2)_n + (v_2)_{n-1}}{2}\right) + \frac{\Phi_4}{\Phi_2}M\left(\frac{(v_1)_n + (v_1)_{n-1}}{2}\right) + \frac{1}{\Phi_1 \Phi_2}K\left(\frac{(v_1)_n + (v_1)_{n-1}}{2}\right) = 0,$$
$$\tag{3.99}$$

$$\left(\frac{t_n - t_{n-1}}{2}\right)\left(1 + \epsilon\left(\frac{\gamma_n + \gamma_{n-1}}{2}\right) + \frac{1}{\Phi_5}PrNr\right) + \epsilon\left(\frac{t_n + t_{n-1}}{2}\right)^2 +$$
$$Pr\frac{\Phi_3}{\Phi_5}\left[\left(\frac{g_n + g_{n-1}}{2}\right)\left(\frac{t_n + t_{n-1}}{2}\right)\right] + Pr\frac{\Phi_3}{\Phi_5}$$
$$\left[-\left(\frac{(v_1)_n + (v_1)_{n-1}}{2}\right)\left(\frac{\gamma_n + \gamma_{n-1}}{2}\right) - A\left\{\left(\frac{\gamma_n + \gamma_{n-1}}{2}\right) + \frac{\chi}{2}\right.\right.$$
$$\left.\left.\left(\frac{t_n + t_{n-1}}{2}\right) = 0.\right.$$
$$\tag{3.100}$$

$$N_G = Re\left[\Phi_5(1+Nr)\left(\frac{t_n - t_{n-1}}{2}\right)^2 + \frac{Br}{\Phi_5\Omega}\left(\frac{(v_1)_n + (v_1)_{n-1}}{2}'^2 + \Phi_1\Phi_4 M v_1^2\right.\right.$$

$$\left.\left.+K\left(\frac{(v_1)_n + (v_1)_{n-1}}{2}'^2\right)\right)\right.$$
$$\tag{3.101}$$

Above non-linear equations are then linearized by using Newton's method. The $(i+1)th$ iterate for above equations can be written as

$$()_n^{(i+1)} = ()_n^{(i)} + \delta()_n^{(i)}, \tag{3.102}$$

by substituting of (3.102) in equations (3.96)-(3.100) and ignoring $O(\delta_n^i) \geqslant 2$, a linear system is obtained as

$$\delta g_n - \delta h_{n-1} - \frac{1}{2}h(\delta(v_1)_n + \delta(v_1)_{n-1}) = (r_1)_{n-\frac{1}{2}}, \tag{3.103}$$

$$\delta(v_1)_n - \delta(v_1)_{n-1} - \frac{1}{2}h(\delta(v_2)_n + \delta(v_2)_{n-1}) = (r_2)_{n-\frac{1}{2}}, \tag{3.104}$$

$$\delta\gamma_n - \delta\gamma_{n-1} - \frac{1}{2}h(\delta t_n + \delta t_{n-1}) = (r_3)_{n-\frac{1}{2}}, \tag{3.105}$$

$$\begin{aligned}(r_4)_{n-\frac{1}{2}} = {}& (c_1)_n\delta g_j + (c_2)_n\delta g_{n-1} + (c_3)_j\delta(v_1)_n + (c_4)_n\delta(v_1)_{n-1} + (c_4)_n\delta(v_1)_{n-1} + (c_5)_n\delta(v_2)_n \\ & + (c_6)_n\delta(v_2)_{n-1} + (c_7)_n\delta\gamma_n + (c_8)_n\delta\gamma_{n-1} + (c_9)_n\delta t_n + (c_{10})_n\delta t_{n-1},\end{aligned} \tag{3.106}$$

$$\begin{aligned}(r_5)_{n-\frac{1}{2}} = {}& (d_1)_n\delta g_n + (d_2)_n\delta g_{n-1} + (d_3)_n\delta(v_1)_n + (d_4)_n\delta(v_1)_{n-1} + (d_5)_n\delta(v_2)_n \\ & + (d_6)_n\delta(v_2)_{n-1} + (d_7)_j\delta\gamma_n + (d_8)_n\delta\gamma_{n-1} + (d_9)_n\delta t_n + (d_{10})_n\delta t_{n-1},\end{aligned} \tag{3.107}$$

where

$$(r_1)_{n-\frac{1}{2}} = -g_n + g_{n-1} + \frac{h}{2}((v_1)_n + (v_1)_{n-1}), \tag{3.108}$$

$$(r_2)_{n-\frac{1}{2}} = -(v_1)_n + (v_1)_{n-1} + \frac{h}{2}((v_2)_n + (v_2)_{n-1}), \tag{3.109}$$

$$(r_3)_{n-\frac{1}{2}} = -\gamma_n + \gamma_{n-1} + \frac{h}{2}(t_n + t_{n-1}), \tag{3.110}$$

$$
\begin{aligned}
(r_4)_{n-\frac{1}{2}} =\ & -h\left[-A\left(\frac{(v_1)_n + (v_1)_{n-1}}{2} + \chi \frac{(v_2)_n - (v_2)_{n-1}}{4} \right) + \left(\frac{(v_1)_n + (v_1)_{n-1}}{2} \right)^2 \right. \\
& \left. -\left(\frac{g_n + g_{n-1}}{2} \right)\left(\frac{(v_2)_n + (v_2)_{n-1}}{2} \right) \right] - h\left[-\frac{1}{\Phi_1\Phi_2}\left(\frac{(v_2)_n - (v_2)_{n-1}}{h} \right) \right. \\
& +\beta\left(\left(\frac{g_n + g_{n-1}}{2} \right)^2 \left(\frac{(v_2)_n - (v_2)_{n-1}}{h} \right) - 2\left(\frac{g_n + g_{n-1}}{2} \right)\left(\frac{(v_1)_n + (v_1)_{n-1}}{2} \right) \right. \\
& \left. \left. \left(\frac{(v_2)_n + (v_2)_{n-1}}{2} \right) \right) \right] - h\left[\frac{\Phi_4}{\Phi_2}M\left(\frac{(v_1)_n + (v_1)_{n-1}}{2} \right) + \frac{1}{\Phi_1\Phi_2}K\left(\frac{(v_1)_n + (v_1)_{n-1}}{2} \right) \right],
\end{aligned}
$$

$$\tag{3.112}$$

$$
\begin{aligned}
(r_5)_{n-\frac{1}{2}} =\ & -h\left[\frac{(t_n - t_{n-1})\left(1 + \epsilon\left(\frac{\gamma_n + \gamma_{n-1}}{2} \right) + \frac{1}{\Phi_5}PrNr \right)}{h} + \epsilon\left(\frac{t_n + t_{n-1}}{2} \right)^2 - \right. \\
& \left. \frac{\Phi_3}{\Phi_5}PrA\left(\frac{\gamma_n + \gamma_{n-1}}{2} + \chi\frac{t_n + t_{n-1}}{2} \right) \right] - h\frac{\Phi_3}{\Phi_5}Pr\left[\left(\frac{(g_n + g_{n-1})(t_n + t_{n-1})}{4} \right) \right. \\
& \left. -\left(\frac{(\gamma_n + \gamma_{n-1})((v_1)_n + (v_1)_{n-1})}{4} \right) \right], \tag{3.113}
\end{aligned}
$$

and boundary conditions are

$$\delta g_0 = 0, \quad (\delta v_1)_0 = 0, \quad \delta t_0 = 0, \quad \delta(v_1)_N = 0, \quad \delta \gamma_N = 0. \tag{3.114}$$

Finally, the coefficient matrix which is known as block tridiagonal matrix is obtained from linearized finite-difference equations. Equations (3.103)-(3.107) can be written as,

$$A\delta = b, \tag{3.115}$$

$$A = \begin{bmatrix} A_1 & C_1 & & & \\ B_2 & A_2 & C_2 & & \\ & \ddots & \ddots & \ddots & \\ & & B_{N-1} & A_{N-1} & C_{N-1} \\ & & & B_N & A_N \end{bmatrix}, \delta = \begin{bmatrix} \delta_1 \\ \delta_2 \\ \vdots \\ \delta_{n-1} \\ \delta_n \end{bmatrix}, b = \begin{bmatrix} (r_1)_{n-\frac{1}{2}} \\ (r_2)_{n-\frac{1}{2}} \\ \vdots \\ (r_{N-1})_{n-\frac{1}{2}} \\ (r_N)_{n-\frac{1}{2}} \end{bmatrix}.$$

$$\tag{3.116}$$

Where A is block tridiagonal matrix of order $N \times N$ with each block size of 5×5. Whereas δ and b are column matrices with N rows. δ is determined by LU factorization [9].

3.4   Results and discussion

Numerical results with discussion are presented in this section in form of graphs and tables. The significant effects of flow governing parameters on fluid motion, temperature and entropy generation profiles are discussed for $Cu-water$ and $TiO_2-water$ nanofluids. Thermo physical properties of Cu and TiO_2 water based nanofluids are

also listed in Table (3.1). Table (3.2) consist of some values of skin friction coefficient and Nusselt number calculated for flow governing parameters at the boundary. All of these results are produced for $\beta = 0.3, \epsilon = 0.1, A = 0.6, M = 0.6, K = 0.6, \Phi = 0.2, \Lambda = 0.1, Nr = 0.2, Pr = 6.2, Br = 5, Re = 5, \Omega = 1, S = 0.2$. In graphs, the behavior of $Cu-$water nanofluid is presented by blue color and the behavior of $TiO_2 - water$ is shown by red color.

Table 3.1: Thermophysical properties

Thermo physical properties	ρ	c_p	k
Pure water (H_2O)	997.1	4179	0.6130
Copper (Cu)	8933	385.0	401.00
Titanium oxide (T_iO_2)	4250	686.2	8.9538

3.4.1 Influence of Maxwell parameter β

Figures (3.1) and (3.2) demonstrated the effects of parameter β on velocity and temperature distribution profiles respectively. Computations are performed for $\beta = 0.01, 0.3, 0.5$ for water based non-Newtonian Maxwell nanofluids. The decay in velocity profile can be seen with increment in β and this reduces the momentum boundary layer thickness. The resistance in fluid is responsible for the decreased fluid motion. Whereas with an increment in Maxwell parameter thermal boundary layer expands, temperature rises due to increase in elasticity stress parameter. Moreover, Figure (3.1) clarifies that the thickness of momentum boundary layer of TiO_2-water is comparatively more than the $Cu-$water nanofluid. Nusselt number for $Cu - water$ and $TiO_2 - water$ decreases in this case. Entropy of system rises

(see Figure 3.3) with increasing values of β.
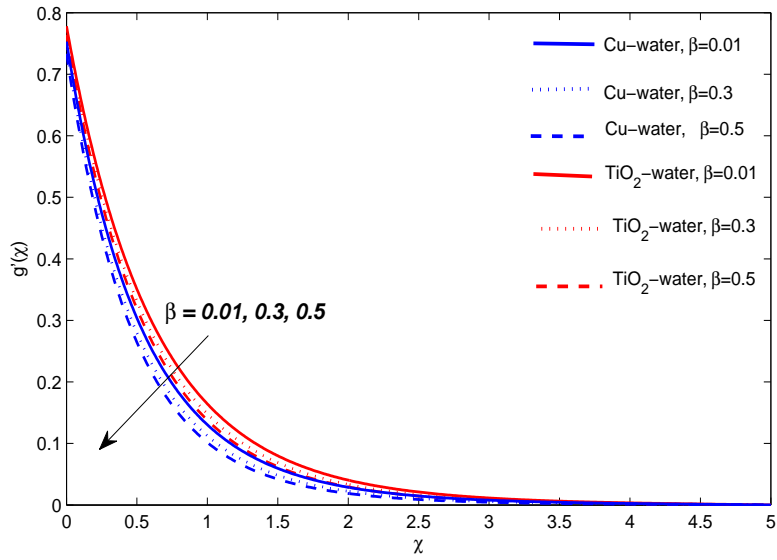
Figure 3.1: Velocity distribution for Maxwell parameter β
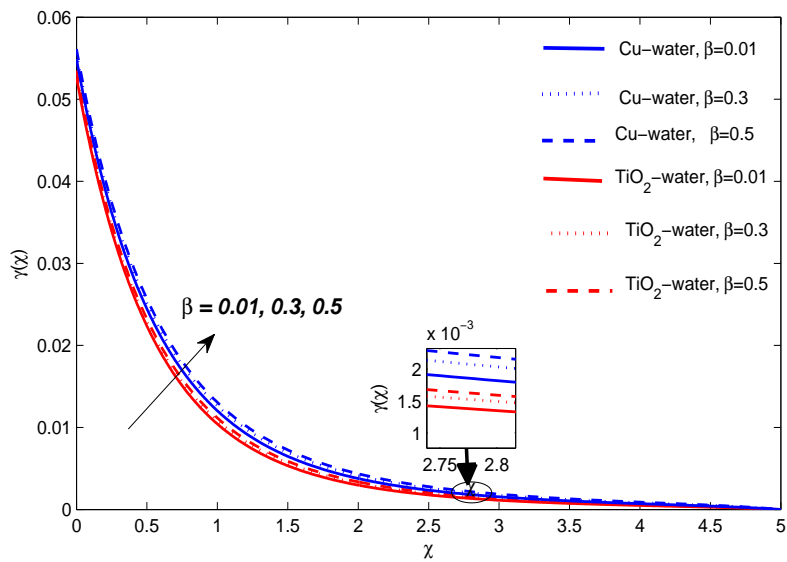
Figure 3.2: Temperature distribution against Maxwell parameter β
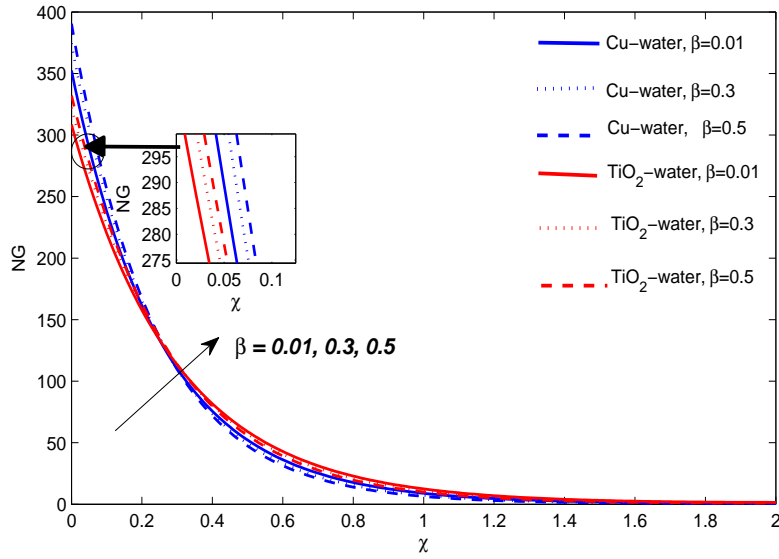
Figure 3.3: Entropy distribution against Maxwell parameter β

3.4.2 Influence of unsteadiness parameter A

Figures (3.4)-(3.5) displayed the nature of velocity and temperature distribution for Maxwell nanofluid. It is noticed that the fluid flows slowly and the temperature decreases with ascending values of A. Reduction in the thermal and momentum boundary layer thickness is noticed for variation in A. Figure (3.4) demonstrated that the momentum boundary layer thickness of TiO_2-water is comparatively more than $Cu-$water nanofluid but the thermal boundary layer of $Cu-$water is wider than TiO_2-water nanofluid. Entropy profile showed cross over point at $\chi = 0.3$, entropy increases before $\chi = 0.3$ and after $\chi = 0.3$ entropy starts decreasing (see Figure (3.6)). It can be claimed that the boundary layer energy is absorbed due to unsteadiness (where the fluid properties are changed with change in time). Finally, the increase in values of the skin friction and the Nusselt numbers is observed for $A = 0.2, 0.6, 1.6$ at the boundary.

40
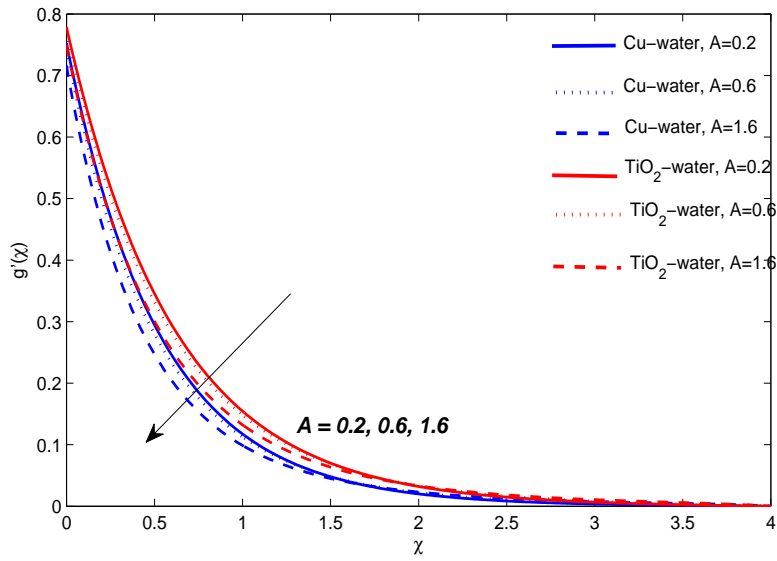
Figure 3.4: Velocity distribution for unsteady parameter A
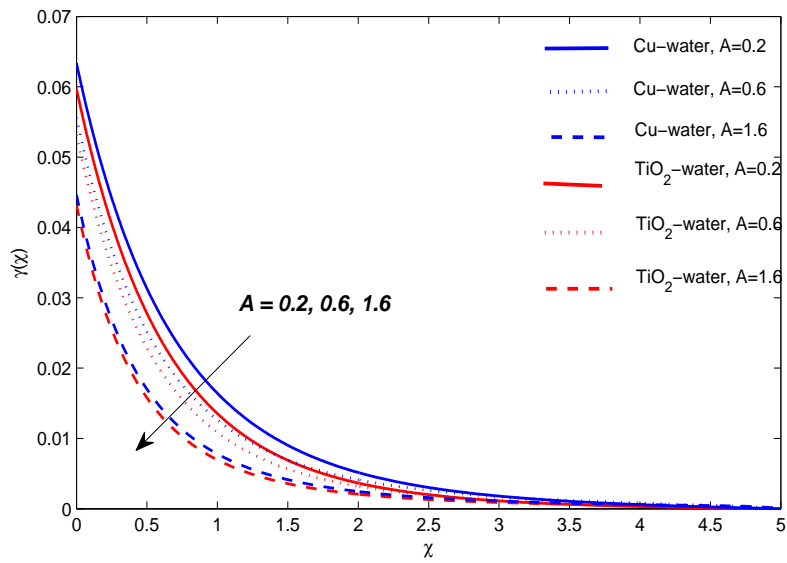
Figure 3.5: Temperature distribution against unsteady parameter A

41
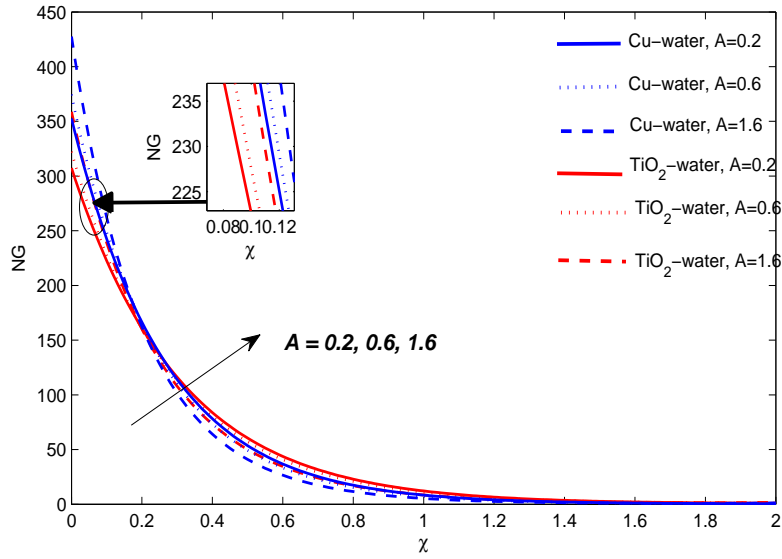
Figure 3.6: Entropy distribution against unsteady parameter A

3.4.3 Influence of magnetic parameter M

The impact of magnetic strength on the nanofluid velocity, temperature and entropy generation profiles are displayed in Figures (3.7)-(3.9) respectively. The decreasing trend in the velocity profile for nanofluid is observed with increasing strength of M, hence the thickness of the momentum boundary layer decreases. The physical reason behind reduction in momentum boundary layer thickness is that; the Lorentz force appears when normally applied magnetic field interacts with electrically conducting nanofluids. As strength of applied magnetic field increases the strength of Lorentz force also increases and acts opposite to fluid motion within the boundary layer and thus the resulting resistance in fluid reduces the thickness of the momentum boundary layer. M is inversely proportional to the density of the nanofluid, so increasing M results in a rise of temperature within boundary layer. Table (3.2) showed that the Nusselt number decreases but the skin friction coefficient increases

by variation of M. Entropy of system increases by increasing magnetic parameter strength.
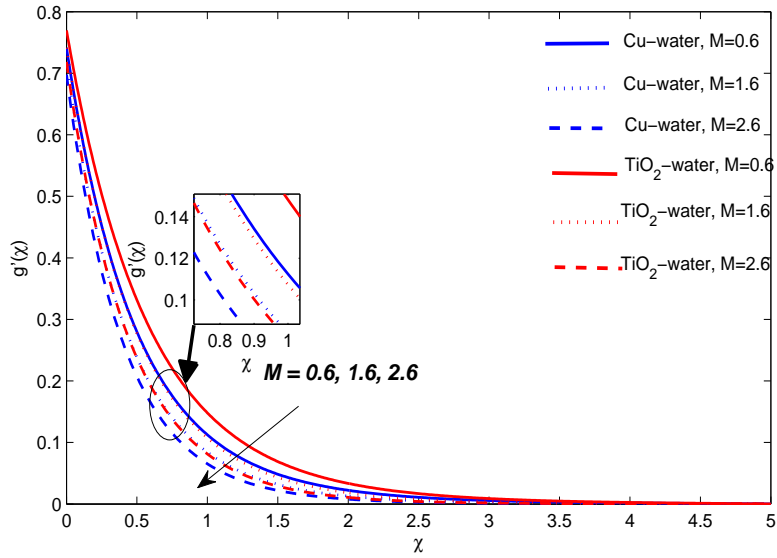
Figure 3.7: Velocity distribution for M
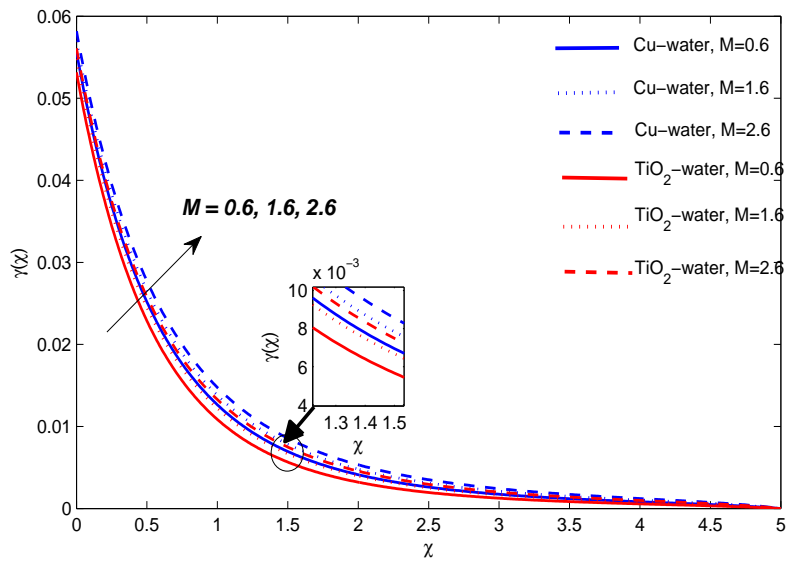
Figure 3.8: Temperature profile for M
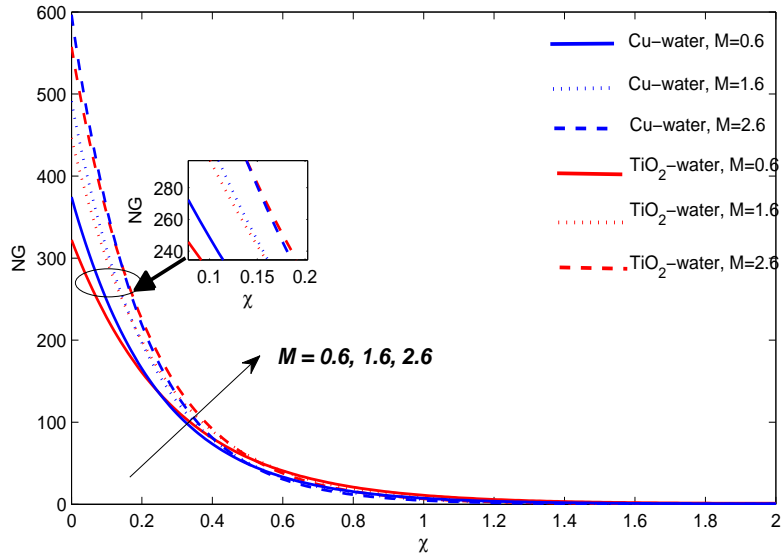
Figure 3.9: Entropy distribution against magnetic parameter M

3.4.4 Influence of porous parameter K

The change in the behaviors of nanofluid velocity and temperature profile are exhibited in Figures (3.10) and (3.11) respectively. These figures are quite similar to the impact of parameter M. Increasing permeability decreases the magnitude of the resistive Darcian body force, therefore a continuous less drag is faced by fluid and the flow reduces so the velocity tends to zero within the boundary layer. The parameter K effects the density of nanofluid directly hence as the permeability of medium is decreased the temperature of fluid within the boundary layer increases, this results in thickness of momentum boundary layer. The temperature also rises within the boundary layer. Entropy of system also rises in this case. Increment in parameter K decreases the heat transfer rate.
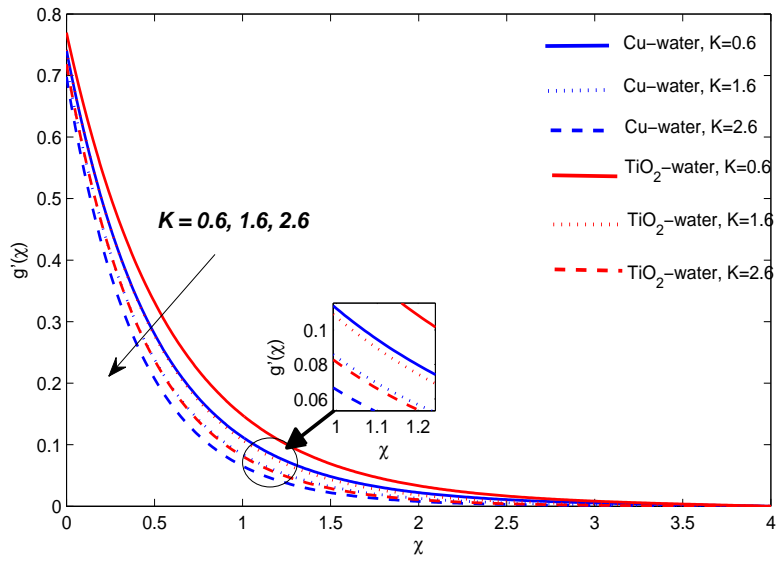
Figure 3.10: Velocity profile for parameter K
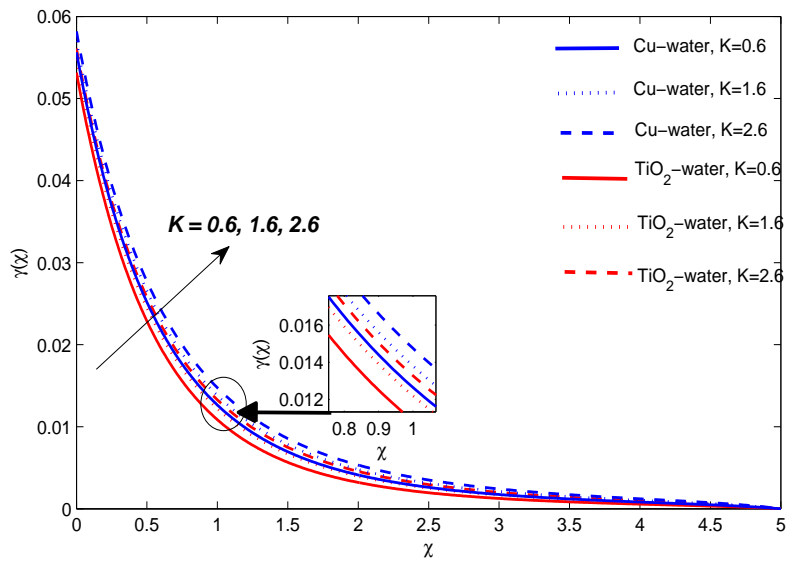
Figure 3.11: Tetmperature distribution against porous parameter K
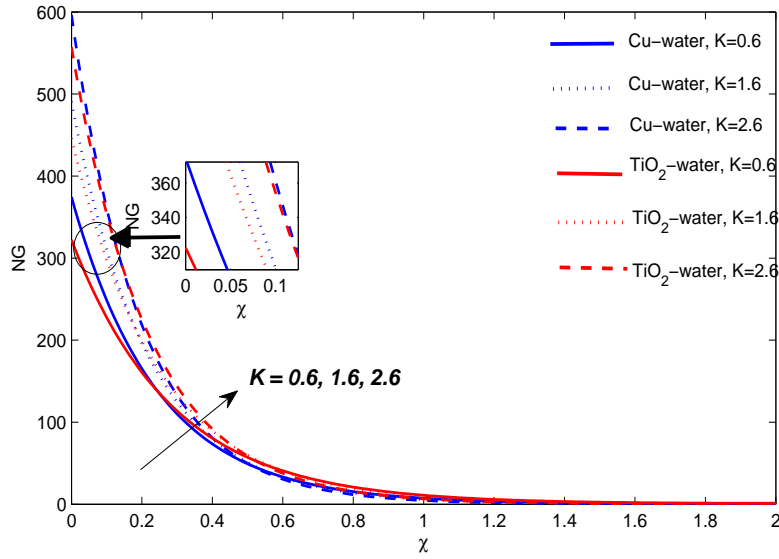
Figure 3.12: Entropy distribution against porous parameter K

3.4.5 Influence of volume concentration parameter Φ

Figures (3.13) and (3.14) displayed the plots of the fluid motion and temperature distribution corresponding to variation in the parameter Φ. Velocity is observed to be decreasing by increasing parameter Φ which results in reduction of momentum boundary layer thickness. The thinning of momentum boundary layer is due to heavy nanoparticle volume fraction. In fact, the thermal conductivity of nanofluids is enhanced due to an increase in the volume of nanoparticles. Thus the momentum boundary layer is shrinked due to an increase in the thermal conductivity. Whereas opposite behavior is observed for temperature profile, thermal boundary layer expands as temperature and thermal conductivity of nanofluid increases. The velocity and temperature gradient at the boundary corresponding to parameter Φ are shown in Table (3.2). Figure (3.15) depicted that the entropy of the system increases by increasing parameter Φ.

46
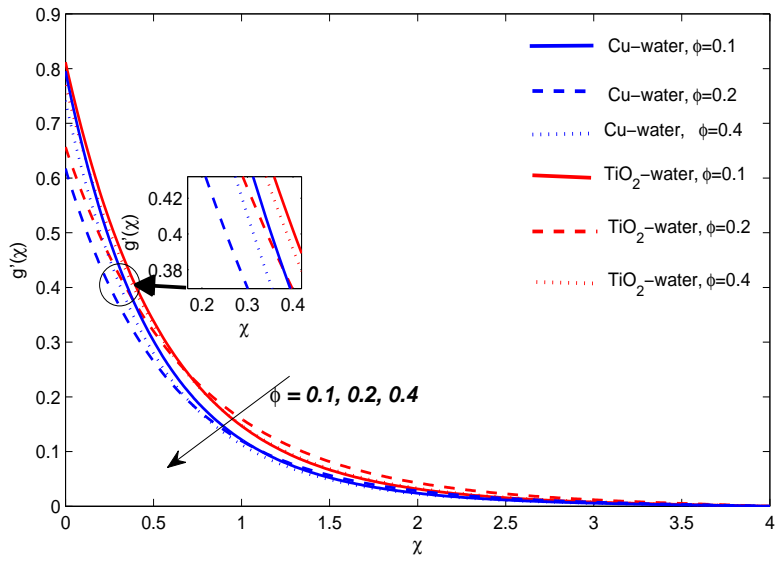
Figure 3.13: Velocity profile for various Φ
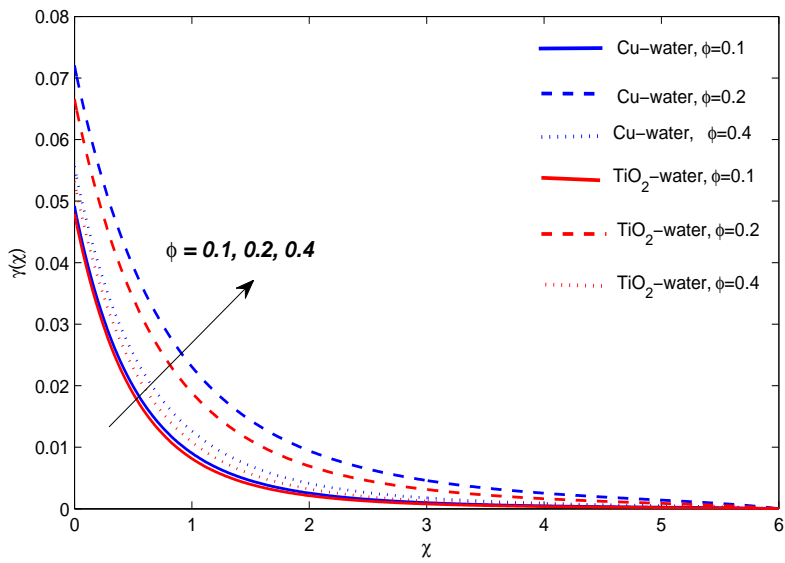
Figure 3.14: Temperature distribution against parameter Φ

47
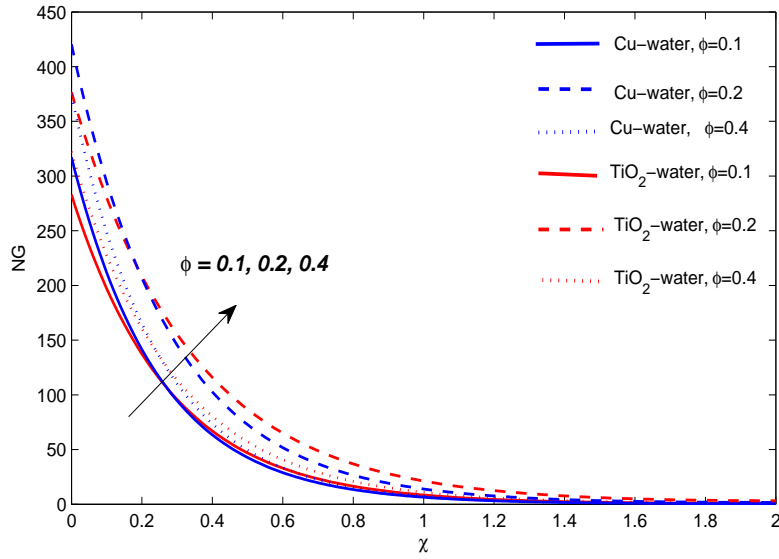
Figure 3.15: Entropy distribution against parameter Φ

3.4.6 Influence of slip parameter Λ

Figures (3.16)-(3.18) demonstrated the influence of variation of slip parameter on fluid motion, temperature distribution and entropy generation profiles for Maxwell nanofluids. Decreasing behavior in velocity profile is observed for slip parameter Λ, it is clear because increase in slip effect retards the fluid flow which slows down the fluid movement. It effects the temperature of fluid oppositely as temperature of nanofluid rises with increase in parameter Λ. The skin friction coefficient decreases due to the fact that slip effects reduces the friction at solid interface of fluid. Here it is significant to distinguish that by increasing the slip velocity the entropy of the system decreases as shown in Figure (3.18).

48
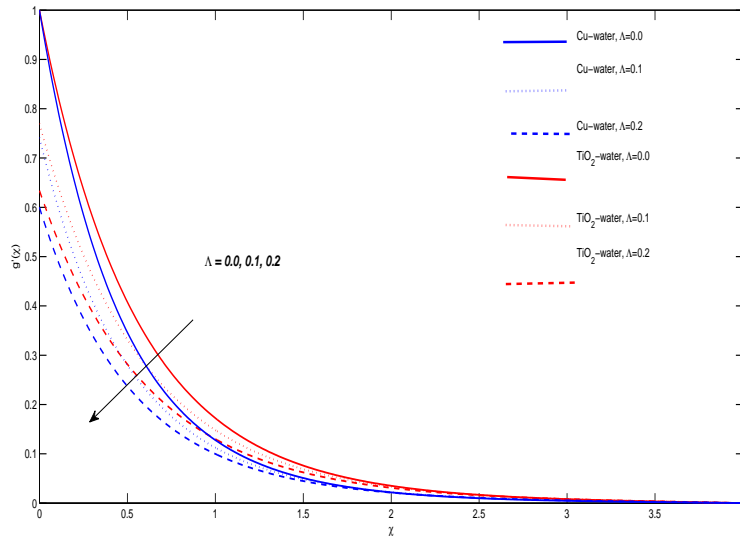
Figure 3.16: Velocity profile for slip effect Λ
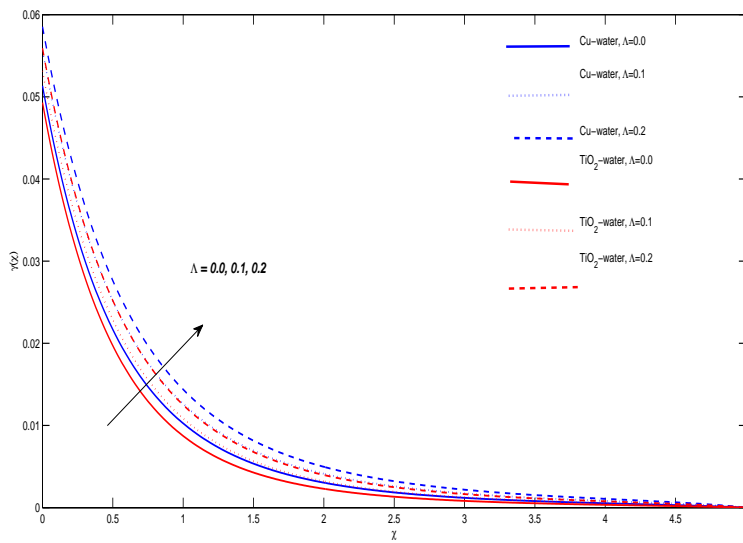
Figure 3.17: Temperature distribution against parameter Λ

49
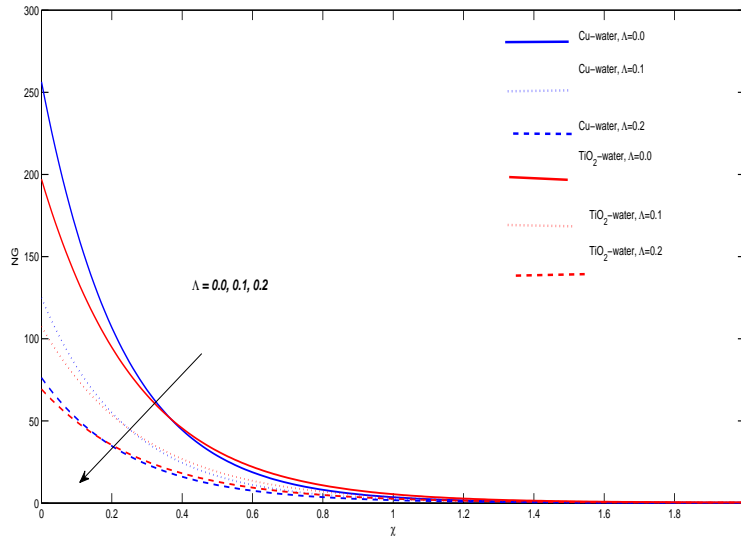
Figure 3.18: Entropy distribution against parameter Λ

3.4.7 Influence of the Brinkmann number Br and Reynolds number Re on the entropy of system

The influence of the Brinkman number (Br) and Reynolds number (Re) on the entropy of the system are presented in Figures (3.19) and (3.20) respectively. It is noticed that the entropy of the system increases rapidly when Reynolds numbers are increased. The physical reason behind this is; at higher Reynolds number the viscous forces are dominated by inertial forces thus system's entropy rises. It is found that the overall entropy of system increases with increment in Brinkman number.
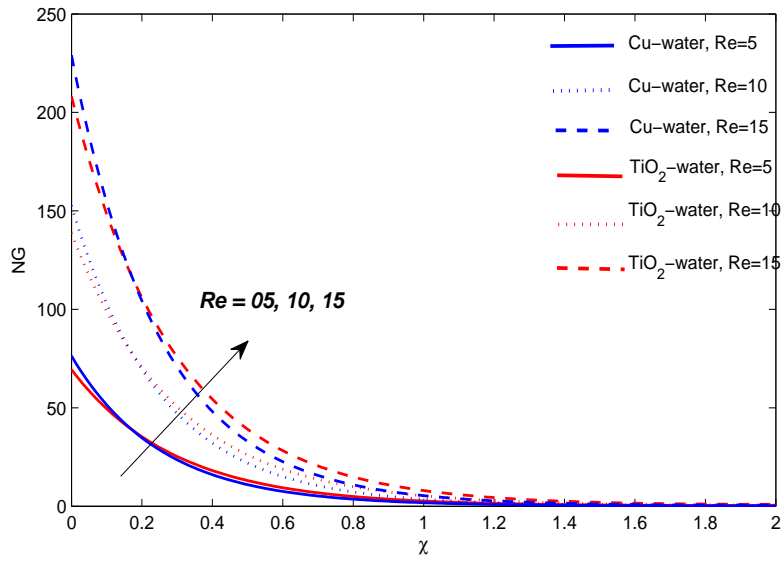
Figure 3.19: Entropy distribution against Re
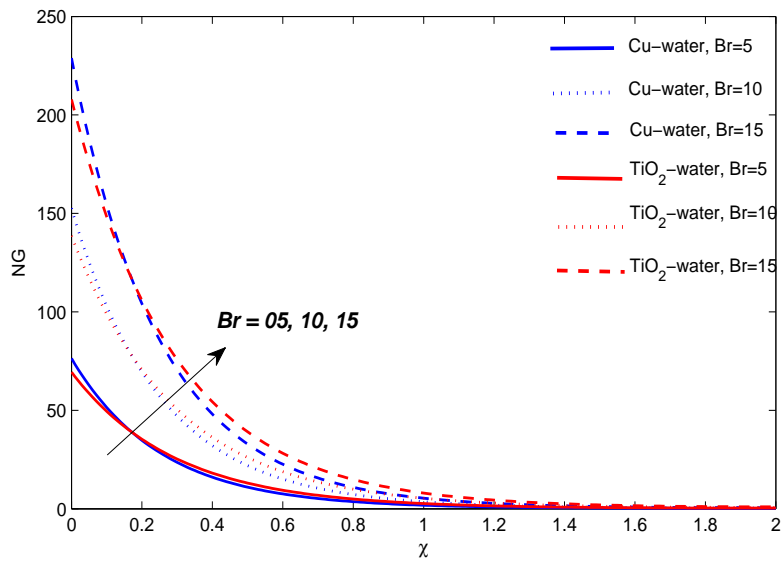
Figure 3.20: Entropy distribution against Br

3.4.8 Effect of flow parameters on Skin friction and Nusselt number

For fixed values of $\epsilon = 0.1$, $Nr = 0.2$, $Bi = 0.1$, $S = 0.2$ and $Pr = 6.2$ some values of the Skin friction and the Nusselt numbers are listed in the following table.

Table 3.2: Calculation of $C_f Re_x^{\frac{1}{2}}$ and $N_u Re_x^{\frac{-1}{2}}$

β	A	M	K	Φ	Λ	$C_f Re_x^{\frac{1}{2}}$ $Cu-$ $water$	$C_f Re_x^{\frac{1}{2}}$ T_iO_2- $water$	$N_u Re_x^{\frac{-1}{2}}$ $Cu-$ $water$	$N_u Re_x^{\frac{-1}{2}}$ T_iO_2- $water$
0.01	0.6	0.6	0.6	0.2	0.1	2.4702	2.2194	0.0650	0.0718
0.3						2.5859	2.3025	0.0649	0.0716
0.5						2.6656	2.3592	0.0648	0.0715
0.3	0.2					2.4713	2.2125	0.0644	0.0711
	0.6					2.5859	2.3025	0.0649	0.0716
	1.6					2.8408	2.5061	0.0657	0.0723
		0.6				2.5859	2.3025	0.0649	0.0716
		1.6				2.8225	2.5862	0.0648	0.0714
		2.6				3.0215	2.8159	0.0647	0.0713
			0.6			2.5859	2.3025	0.0649	0.0716
			1.6			2.8221	2.5858	0.0648	0.0714
			2.6			3.0290	2.8152	0.0647	0.0713
				0.1		2.0461	1.8795	0.0857	0.0901
				0.2		2.5859	2.3025	0.0649	0.0716
				0.4		2.8253	3.4338	0.0373	0.0455
					0.0	3.7682	3.1669	0.0652	0.0718
					0.1	2.5859	2.3025	0.0649	0.0716
					0.2	1.9998	1.8309	0.0647	0.0713

Chapter 4

Heat Transfer and Entropy Analysis of Maxwell Nanofluid Flow over a Stretching Flat Surface

In this chapter, the work presented in the previous Chapter has been extended by including the viscous dissipation effects in the model. The current work deals with the non-Newtonian Maxwell nanofluid flow on stretching sheet. Suitable similarity transformation are employed to transform nonlinear partial differential equations of conservation of mass, momentum, energy and entropy into ordinary differential equations. The solution of transformed ordinary differential equations is acquired by using the Keller-box method. The numerical computations are performed to calculate the skin-friction coefficient and the local Nusselt number for Copper and Titanium water based nanofluids. Finally, the numerical results are presented along with discussion for the significant effect of different governing flow parameters on velocity, temperature and entropy generation profiles of considered nanofluid.

The physical model and governing partial differential equations are presented in Section 4.1. Similarity transformations and reduction of governing partial differential equations to a system of non-linear ordinary differential equations are given in Section 4.2. Section 4.3 is about the details of numerical method that we have used for the numerical computations. Finally, the numerically computed results and their discussion in the form of graphs and tables are presented in Section 4.4 .

4.1 Mathematical model

In present work, an unsteady, two-dimensional laminar flow of a Maxwell nanofluid with heat transfer characteristics is considered over the porous stretching sheet. The incompressible electrically conducting flow is taken under the effects of viscous dissipation and constant thermal conductivity. Stretching velocity, wall temperature and magnetic field are considered same as in previous Chapter.
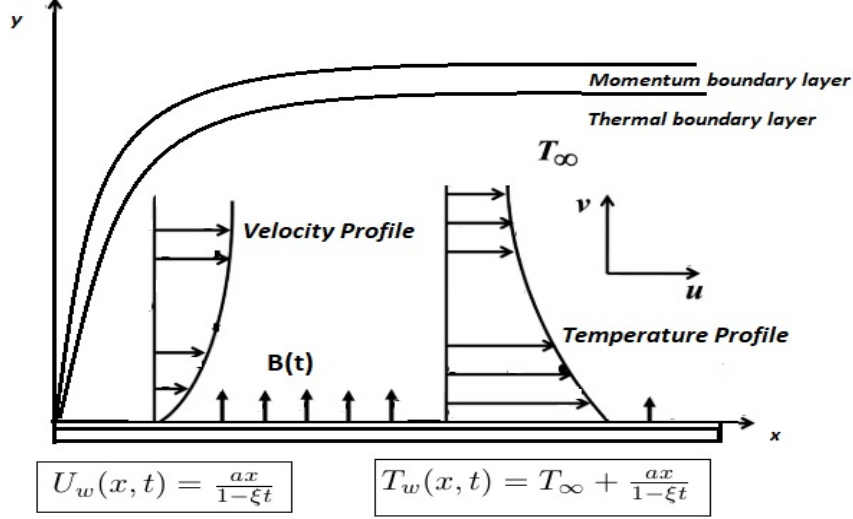
Figure 4.1: Schematic diagram of fluid flow

The continuity, momentum, energy and entropy equations described in [17] are modified for the unsteady two-dimensional laminar flow with thermal constant thermal conductivity, viscous dissipation and MHD effects are given as

$$\frac{\partial v_1}{\partial x} + \frac{\partial v_2}{\partial y} = 0, \tag{4.1}$$

$$\frac{\partial v_1}{\partial t} + v_1\frac{\partial v_1}{\partial x} + v_2\frac{\partial v_1}{\partial y} = \frac{\mu_{nf}}{\rho_{nf}}\frac{\partial^2 v_1}{\partial y^2} - \lambda\left[v_1^2\frac{\partial^2 v_1}{\partial x^2} + v_2^2\frac{\partial^2 v_1}{\partial y^2} + 2v_1v_2\frac{\partial^2 v_1}{\partial x\partial y}\right] - \frac{\sigma_{nf}B^2(t)v_1}{\rho_{nf}}, \tag{4.2}$$

$$\frac{\partial T}{\partial t} + v_1\frac{\partial T}{\partial x} + v_2\frac{\partial T}{\partial y} = \frac{\kappa_{nf}}{(\rho C_p)_{nf}}\left[\frac{\partial^2 T}{\partial y^2}\right] - \frac{1}{(\rho C_p)_{nf}}\left(\frac{\partial q_r}{\partial y}\right) + \frac{\mu_{nf}}{(\rho C_p)_{nf}}\left(\frac{\partial v_1}{\partial y}\right)^2, \tag{4.3}$$

$$E_G = \frac{k_{nf}}{T_\infty^2}\left\{\left(\frac{\partial T}{\partial y}\right)^2 + \frac{16\sigma^* T_\infty^3}{3k^*}\left(\frac{\partial T}{\partial y}\right)^2\right\} + \frac{\mu_{nf}}{T_\infty}\left(\frac{\partial v_1}{\partial y}\right)^2 + \frac{\sigma_{nf}B_o^2(t)v_1^2}{T_\infty}. \tag{4.4}$$

56

The following boundary conditions are assumed for the investigated problem

$$v_1(x,0,t) = U_w + W_1\mu_{nf}\Big(\frac{\partial v_1}{\partial y}\Big), \quad v_2(x,0,t) = V_w, \quad -\kappa_f(\frac{\partial T}{\partial y}) = h_f(T_w - T), \ (4.5)$$

$$v_1 \longrightarrow 0, \quad T \longrightarrow T_\infty \ \ as \ \ y \longrightarrow \infty \ . \tag{4.6}$$

Variables appearing in above equations are already defined in Chapter 3.

4.2 Similarity Transformation

In order to find the solution of boundary value problem (BVP) (4.1) - (4.6) , initially similarity technique is employed to transform governing governing partial differential equations into ordinary differential equations. Using similarity transformation defined in equations (3.7) - (3.8) into equations (4.1) - (4.6). The similarity transformation eliminates the continuity equation and reduce the other equations into odes. Calculating derivatives in order to determine the equations for the similarity solution of the problem.

Letting,

$$v_1 = \frac{\partial \psi}{\partial y}, \tag{4.7}$$

$$v_1 = \frac{\partial \psi}{\partial \chi}.\frac{\partial \chi}{\partial y}, \tag{4.8}$$

$$\chi(x,y,t) = \sqrt{\frac{a}{\nu_f(1-\xi t)}}y, \tag{4.9}$$

Differentiating w. r. t. 'y',

$$\frac{\partial \chi}{\partial y} = \sqrt{\frac{a}{\nu_f(1-\xi t)}}, \tag{4.10}$$

$$\psi(x, y, t) = \sqrt{\frac{\nu_f a}{(1 - \xi t)}} x f(\chi), \tag{4.11}$$

$$\frac{\partial \psi}{\partial y} = \sqrt{\frac{\nu_f a}{(1 - \xi t)}} x g'(\chi) \left(\frac{\partial \chi}{\partial y} \right), \tag{4.12}$$

$$\frac{\partial \psi}{\partial y} = \frac{ax}{(1 - \xi t)} g'(\chi), \tag{4.13}$$

which gives,

$$v_1 = \frac{ax}{(1 - \xi t)} g'(\chi). \tag{4.14}$$

Now, we aim to find,

$$\frac{\partial v_1}{\partial x} = \frac{a}{(1 - \xi t)} g'(\chi). \tag{4.15}$$

Calculating v_2,

$$v_2 = -\frac{\partial \psi}{\partial x}, \tag{4.16}$$

Differentiating w. r. t. 'x',

$$\frac{\partial \psi}{\partial x} = \sqrt{\frac{\nu_f a}{(1 - \xi t)}} g(\chi), \tag{4.17}$$

we get expression for v_2,

$$v_2 = -\sqrt{\frac{\nu_f a}{(1 - \xi t)}} f(\chi). \tag{4.18}$$

$$\frac{\partial v_2}{\partial y} = -\sqrt{\frac{\nu_f a}{(1 - \xi t)}} g'(\chi) \left(\frac{\partial \chi}{\partial y} \right), \tag{4.19}$$

$$\frac{\partial v_2}{\partial y} = -\frac{a}{(1 - \xi t)} f'(\chi), \tag{4.20}$$

$$\frac{\partial v_1}{\partial x} + \frac{\partial v_2}{\partial y} = \frac{a}{(1 - \xi t)} g'(\chi) - \frac{a}{(1 - \xi t)} g'(\chi) = 0. \tag{4.21}$$

58

$$\frac{\partial v_1}{\partial t} = \frac{\partial}{\partial t}\left(\frac{ax}{(1-\xi t)}g'(\chi)\right), \tag{4.22}$$

$$\frac{\partial v_1}{\partial t} = \frac{ax}{(1-\xi t)^2}\left[\xi g' + \frac{\xi g''}{2}\right], \tag{4.23}$$

$$\frac{\partial v_1}{\partial x} = \frac{a}{(1-\xi t)}g'(\chi), \tag{4.24}$$

$$v_1\frac{\partial v_1}{\partial x} = \frac{ax}{(1-\xi t)}g'(\chi)\left(\frac{a}{(1-\xi t)}g'(\chi)\right), \tag{4.25}$$

$$v_1\frac{\partial v_1}{\partial x} = \frac{a^2 x}{(1-\xi t)^2}g'^2(\chi), \tag{4.26}$$

$$\frac{\partial v_1}{\partial y} = \frac{axg''(\chi)}{(1-\xi t)}\sqrt{\frac{a}{\nu_f(1-\xi t)}}, \tag{4.27}$$

$$v_2\frac{\partial v_1}{\partial y} = -\sqrt{\frac{\nu_f a}{(1-\xi t)}}g(\chi)\left(axg''(\chi)\sqrt{\frac{a}{\nu_f(1-\xi t)}}y\right), \tag{4.28}$$

$$v_2\frac{\partial v_1}{\partial y} = -\frac{a^2 xg(\chi)g''(\chi)}{(1-\xi t)^2}. \tag{4.29}$$

$$\frac{\partial v_1}{\partial t} + v_1\frac{\partial v_1}{\partial x} + v_2\frac{\partial v_1}{\partial y} = \frac{a^2 xg}{(1-\xi t)^2}\left[A(g' + \frac{\chi}{2}g'' + g'^2 - gg'')\right]. \tag{4.30}$$

where $A = \frac{\xi}{a}$. Now, solving the following term from equation (4.2).

$$= \lambda\left[(v_1)^2\frac{\partial^2 v_1}{\partial x^2} + (v_2)^2\frac{\partial^2 v_1}{\partial y^2} + 2v_1 v_2\frac{\partial^2 v_1}{\partial x\partial y}\right], \tag{4.31}$$

Calculating derivatives in sequence,

$$\frac{\partial^2 v_1}{\partial y^2} = \frac{\partial}{\partial y}\left(\frac{axg''(\chi)}{(1-\xi t)}\sqrt{\frac{a}{\nu_f(1-\xi t)}}\right), \tag{4.32}$$

$$\frac{\partial^2 v_1}{\partial y^2} = \left(\frac{axg'''(\chi)}{(1-\xi t)}\sqrt{\frac{a}{\nu_f(1-\xi t)}}\right)\frac{\partial \chi}{\partial y}, \tag{4.33}$$

$$\frac{\partial^2 v_1}{\partial y^2} = \left(\frac{a^2 x g'''(\chi)}{(1-\xi t)^2 \nu_f}\right), \tag{4.34}$$

$$\frac{\partial^2 v_1}{\partial x^2} = 0, \tag{4.35}$$

$$\frac{\partial^2 v_1}{\partial x \partial y} = \left(\frac{ag''(\chi)}{(1-\xi t)}\sqrt{\frac{a}{\nu_f(1-\xi t)}}\right) \tag{4.36}$$

$$2v_1 v_2 = 2\left(\frac{ax}{(1-\xi t)}g'(\chi)\right)\left(-\sqrt{\frac{\nu_f a}{(1-\xi t)}}g(\chi)\right), \tag{4.37}$$

$$2v_1 v_2 \left(\frac{\partial^2 v_1}{\partial x \partial y}\right) = \frac{-2a^3 gg'g''x}{(1-\xi t)^3}, \tag{4.38}$$

$$(v_1)^2 = \frac{a^2 x^2 g'^2(\chi)}{(1-\xi t)^2}, \tag{4.39}$$

$$(v_1)^2 \left(\frac{\partial^2 v_1}{\partial x^2}\right) = 0, \tag{4.40}$$

$$(v_2)^2 = \frac{\nu_f a g^2(\chi)}{(1-\xi t)}, \tag{4.41}$$

$$(v_2)^2 \frac{\partial^2 v_1}{\partial y^2} = \frac{xa^3 g^2(\chi)g'''(\chi)}{(1-\xi t)^3}, \tag{4.42}$$

$$\lambda\left[(v_1)^2\frac{\partial^2(v_1)}{\partial x^2} + (v_1)^2\frac{\partial^2 v_1}{\partial y^2} + 2v_1 v_2\frac{\partial^2 v_1}{\partial x \partial y}\right] = \lambda\left[0 + \frac{xa^3 g^2(\chi)g'''(\chi)}{(1-\xi t)^3} - \frac{2a^3 gg'g''x}{(1-\xi t)^3}\right], \tag{4.43}$$

$$\lambda\left[(v_1)^2\frac{\partial^2 v_1}{\partial x^2} + (v_2)^2\frac{\partial^2 v_1}{\partial y^2} + 2v_1 v_2\frac{\partial^2 v_1}{\partial x \partial y}\right] = -\frac{\lambda_o a^3 x}{(1-\xi t)^2}\left(g^2 g''' - 2gg'g''\right). \tag{4.44}$$

Now solving remaining terms of equation (4.2)

$$= \frac{\mu_{nf}}{\rho_{nf}}\left(\frac{\partial^2 v_1}{\partial y^2}\right) - \frac{\sigma_{nf}B^2(t)v_1}{\rho_{nf}}, \tag{4.45}$$

$$= \frac{\mu_{nf}}{\rho_{nf}}\left(\left(\frac{a^2 x g'''(\chi)}{(1-\xi t)^2 \nu_f}\right)\right) - \frac{\sigma_{nf}B^2(t)}{\rho_{nf}}\left(\frac{ax}{(1-\xi t)}g'(\chi)\right), \tag{4.46}$$

$$= \frac{a^2 x}{(1-\xi t)^2}\left[\frac{\mu_f g'''}{\rho_f \Phi_1 \Phi_2 \nu_f} - \frac{\sigma_f \Phi_4 B_o^2 g'}{\rho_f \Phi_2}a\right], \tag{4.47}$$

$$\frac{\mu_{nf}}{\rho_{nf}}\left(\frac{\partial^2 u}{\partial y^2}\right) - \frac{\sigma_{nf}B^2(t)u}{\rho_{nf}} - \frac{\mu_{nf}}{\rho_{nf}k}u = \frac{a^2 x}{(1-\xi t)^2}\left[\frac{g'''}{\Phi_1 \Phi_2} - \frac{\Phi_4}{\Phi_2}Mg'\right], \tag{4.48}$$

Inserting (4.30), (4.44) and (4.48) in (4.2), yields the ODE

$$A\left(\frac{\chi}{2}g'' + g'\right) + g'^2 - gg'' - \frac{g'''}{\Phi_1 \Phi_2} + \beta\left(g^2 g''' - 2gg'g''\right) + \frac{\Phi_4}{\Phi_2}Mg' = 0. \tag{4.49}$$

Using the next transformation,

$$\gamma(\chi) = \frac{T - T_\infty}{T_w - T_\infty} \tag{4.50}$$

$$T_w - T_\infty = \frac{ax}{(1-\xi t)} \tag{4.51}$$

$$\gamma(\chi)\frac{ax}{(1-\xi t)} = (T - T_\infty) \tag{4.52}$$

$$T = T_\infty + \frac{ax}{(1-\xi t)}\gamma(\chi) \tag{4.53}$$

Differentiating above expression w. r. t. 'x', 'y' and 't',

$$\frac{\partial T}{\partial x} = \frac{a}{(1 - \xi t)}\gamma(\chi), \tag{4.54}$$

$$v_1 \left(\frac{\partial T}{\partial x}\right) = \left(\frac{ax}{(1 - \xi t)}g'(\chi)\right)\frac{a}{(1 - \xi t)}\gamma(\chi), \tag{4.55}$$

$$\frac{\partial T}{\partial y} = \frac{ax}{(1 - \xi t)}\gamma'(\chi)\left(\frac{\partial \chi}{\partial y}\right) \tag{4.56}$$

$$\frac{\partial T}{\partial y} = \frac{ax}{(1 - \xi t)}\gamma'(\chi)\sqrt{\frac{a}{\nu_f(1 - \xi t)}}, \tag{4.57}$$

$$v_2 \left(\frac{\partial T}{\partial y}\right) = \left(-\sqrt{\frac{\nu_f a}{(1 - \xi t)}}g(\chi)\right)\frac{ax}{(1 - \xi t)}\gamma'(\chi)\sqrt{\frac{a}{\nu_f(1 - \xi t)}} \tag{4.58}$$

$$\frac{\partial T}{\partial t} = \frac{\xi ax}{(1 - \xi t)^2} + \frac{ax}{(1 - \xi t)}\gamma'(\chi)\left(\frac{\partial \chi}{\partial t}\right) \tag{4.59}$$

$$\frac{\partial T}{\partial t} = \frac{\xi ax}{(1 - \xi t)^2} + \frac{ax}{(1 - \xi t)}\gamma'(\chi)\left(\sqrt{\frac{1}{\nu_f(1 - \xi t)}}y\left(\frac{\xi}{1 - \xi t}\frac{1}{2}\right)\right) \tag{4.60}$$

$$\frac{\partial T}{\partial t} = \frac{\xi ax}{(1 - \xi t)^2} + \frac{\xi ax}{2(1 - \xi t)^2}\gamma'(\chi), \tag{4.61}$$

$$\frac{\partial T}{\partial t} = \frac{\xi ax}{(1 - \xi t)^2}\left(\gamma(\chi) + \frac{\chi}{2}\gamma'(\chi)\right) \tag{4.62}$$

$$\frac{\partial T}{\partial t} = \frac{\xi a^2 x}{a(1 - \xi t)^2} \left(\gamma(\chi) + \frac{\chi}{2}\gamma'(\chi) \right) \tag{4.63}$$

$$\frac{\partial T}{\partial t} = \frac{a^2 x}{(1 - \xi t)^2} A \left(\gamma(\chi) + \frac{\chi}{2}\gamma'(\chi) \right) \tag{4.64}$$

$$\frac{\partial T}{\partial t} + v_1 \frac{\partial T}{\partial x} + v_2 \frac{\partial T}{\partial y} = \frac{a^2 x}{(1 - \xi t)^2} A \left(\gamma(\chi) + \frac{\chi}{2}\gamma'(\chi) \right) + \left(\frac{ax}{(1 - \xi t)}g'(\chi) \right) \frac{a}{(1 - \xi t)}\gamma(\chi)$$
$$- \left(\sqrt{\frac{\nu_f a}{(1 - \xi t)}}g(\chi) \right) \frac{ax}{(1 - \xi t)}\gamma'(\chi)\sqrt{\frac{a}{\nu_f(1 - \xi t)}} \tag{4.65}$$

Left hand side of equation (4.3) is given by,

$$\frac{\partial T}{\partial t} + v_1 \frac{\partial T}{\partial x} + v_2 \frac{\partial T}{\partial y} = \frac{a^2 x}{(1 - \xi t)^2} \left[A(\gamma + \frac{\chi}{2}\gamma') + \gamma g' - \gamma' g \right]. \tag{4.66}$$

Now, solving the other side of equation (4.3)

$$\frac{\mu_{nf}}{(\rho C_p)_{nf}} \left(\frac{\partial v_1}{\partial y} \right)^2 = \frac{\Phi_1}{\Phi_5} E_c g''^2, \tag{4.67}$$

$$\frac{1}{(\rho C_p)_{nf}} \left(\frac{\partial^2 T}{\partial y^2} \right) = \frac{1}{(\rho C_p)_{nf}} \frac{a^2 x}{\nu_f(1 - \xi t)^2}, \tag{4.68}$$

$$-\frac{1}{(\rho C_p)_{nf}} \left[\frac{\partial q_r}{\partial y} \right] = -\frac{1}{(\rho C_p)_{nf}} \frac{-16\sigma^* T^3}{3k^*} \left(\frac{\partial^2 T}{\partial y^2} \right), \tag{4.69}$$

$$\left(\frac{\partial^2 T}{\partial y^2} \right) = \frac{a^2 x}{\nu_f(1 - \xi t)^2}, \tag{4.70}$$

$$\frac{1}{(\rho C_p)_{nf}} \left[\frac{\partial q_r}{\partial y} \right] = \frac{a^2 x}{\nu_f(1 - \xi t)^2} \left[\frac{16\sigma^* T^3}{3k^* \nu_f \rho C_p)_f} \frac{\gamma''}{\Phi_3} \right], \tag{4.71}$$

63

$$\frac{1}{(\rho C_p)_{nf}} \left[\frac{\partial q_r}{\partial y} \right] = \frac{a^2 x}{(1 - \xi t)^2} \left[\frac{Nr\gamma''}{\Phi_3} \right]. \tag{4.72}$$

$$\left[A\left(\gamma + \frac{\chi}{2}\gamma'\right) + \gamma g' - \gamma' g \right] - \frac{\Phi_5}{\Phi_3} \frac{1}{Pr} \left[1 + \gamma'' + \frac{\Phi_1}{\Phi_5} E_c g_2'' \right] - \left[\frac{Nr\gamma''}{\Phi_3} \right], \tag{4.73}$$

Inserting (4.66), (**??**) and (4.72) in (4.3), yields the following ODE

$$\gamma'' \left(1 + \frac{1}{\Phi_5} Pr Nr \right) + Pr \frac{\Phi_3}{\Phi_5} \left[g\gamma' - g'\gamma - A\left(\gamma + \frac{\chi}{2}\gamma'\right) + \frac{\Phi_1}{\Phi_3} E_c g_2'' \right] = 0. \tag{4.74}$$

$$N_G = Re \left[\Phi_5 (1 + Nr)\gamma'^2 + \frac{Br}{\Phi_5 \omega} \left(g''^2 + \Phi_1 \Phi_4 M g'^2 \right) \right]. \tag{4.75}$$

with

$$g(0) = S, \quad g'(0) = 1 + \frac{\Lambda}{\Phi_1} g''(0), \quad \gamma'(0) = -B_i(1 - \gamma(0)), \tag{4.76}$$

$$g'(\chi) \longrightarrow 0, \quad \gamma(\chi) \longrightarrow 0 \ \ as \ \ \chi \longrightarrow \infty. \tag{4.77}$$

Where $E_c = \frac{U_W^2}{(C_p)_f (T_w - T_\infty)}$ is the Eckert number and all other governing parameters are given in Chapter 3.

4.3 Finding Numerical Solution

Non-similar solution of equations (4.49),(4.74) and (4.75) with subject to conditions, (4.76)-(4.77) is found by Keller-box method. In order to apply the Keller-box method first write the equations (4.49), (4.74) and (4.77) as a system of six first-order ordinary differential equations with some newly introduced variables, reduced equations are

$$v_1 = g', \tag{4.78}$$

$$v_2 = v_1', \tag{4.79}$$

$$t = \gamma', \tag{4.80}$$

$$A\left(\frac{\chi}{2}v_2 + v_1\right) + v_1^2 - gv_2 - \frac{v_2'}{\Phi_1\Phi_2} + \beta(g^2v_2 - 2gv_1v_2) + \frac{\Phi_4}{\Phi_2}Mv_1 = 0, \tag{4.81}$$

$$t'\left(1 + \frac{1}{\Phi_5}PrNr\right) + Pr\frac{\Phi_3}{\Phi_5}\left[gt - v_1\gamma - A\left(\gamma + \frac{\chi}{2}t\right) + \frac{\Phi_1}{\Phi_3}E_cv_2^2\right] = 0, \tag{4.82}$$

$$N_G = Re\left[\Phi_5(1 + Nr)t^2 + \frac{Br}{\Phi_5\Omega}\left(v_1'^2 + \Phi_1\Phi_4Mv_1^2\right)\right] \tag{4.83}$$

and conditions are

$$g(0) = S, \quad v_1(0) = 1 + \frac{\Lambda}{\phi_1}v_2(0), \quad t(0) = -B_i(1 - \gamma(0)), \tag{4.84}$$

$$v_1(\infty) \longrightarrow 0, \quad \gamma(\infty) \longrightarrow 0. \tag{4.85}$$

After obtaining first-order system, discretize the domain which allows to calculate the approximate solution over each sub domain rather then over entire domain.

$$\chi_0 = 0; \quad \chi_n = \chi_{n-1} + h, \quad n = 1, 2, 3, ..., N - 1; \quad \chi_N = \chi_\infty.$$

Then difference equations are obtained using backward differences. Functions are replaced with their mean averages. The system of ordinary differential (??)-(4.75) is then converted into the following non-linear algebraic equations.

$$\frac{(v_1)_n + (v_1)_{n-1}}{2} = \frac{g_n - g_{n-1}}{h}, \tag{4.86}$$

$$\frac{(v_2)_n + (v_2)_{n-1}}{2} = \frac{(v_1)_n - (v_1)_{n-1}}{h}, \tag{4.87}$$

$$\frac{t_n + t_{n-1}}{2} = \frac{\gamma_n - \gamma_{n-1}}{h}, \tag{4.88}$$

65

$$A\left\{\left(\frac{(v_1)_n + (v_1)_{n-1}}{2}\right) + \frac{\chi}{2}\left(\frac{(v_2)_n + (v_2)_{n-1}}{2}\right)\right\} + \left(\frac{(v_1)_n + (v_1)_{n-1}}{2}\right)^2 -$$

$$\left(\frac{g_n + g_{n-1}}{2}\right)\left(\frac{(v_2)_n + (v_2)_{n-1}}{2}\right) - \frac{1}{\Phi_1\Phi_2}\left(\frac{(v_2)_n - (v_2)_{n-1}}{h}\right) +$$

$$\beta\left(\left(\frac{g_n + g_{n-1}}{2}\right)^2\left(\frac{(v_2)_n - (v_2)_{n-1}}{h}\right) - 2\left(\frac{g_n + g_{n-1}}{2}\right)\left(\frac{(v_1)_n + (v_1)_{n-1}}{2}\right)\right) \qquad (4.89)$$

$$\left(\frac{(v_2)_n + (v_2)_{n-1}}{2}\right) + \frac{\Phi_4}{\Phi_2}M\left(\frac{(v_1)_n + (v_1)_{n-1}}{2}\right) = 0,$$

$$\left(\frac{t_n - t_{n-1}}{h}\right) + \frac{1}{\Phi_5}PrNr + Pr\frac{\Phi_3}{\Phi_5}\left[\left(\frac{g_n + g_{n-1}}{2}\right)\left(\frac{t_n + t_{n-1}}{2}\right)\right]$$

$$+Pr\frac{\Phi_3}{\Phi_5}\left[-\left(\frac{(v_1)_n + (v_1)_{n-1}}{2}\right)\left(\frac{\gamma_n + \gamma_{n-1}}{2}\right) - A\left\{\left(\frac{\gamma_n + \gamma_{n-1}}{2}\right)\right.\right. \qquad (4.90)$$

$$\left.+\frac{\chi}{2}\left(\frac{t_n + t_{n-1}}{2}\right)\right) = 0.$$

$$N_G = Re\left[\Phi_5(1 + Nr)\left(\frac{t_n - t_{n-1}}{2}\right)^2 + \frac{Br}{\Phi_5\Omega}\left(\frac{(v_1)_n + (v_1)_{n-1}}{2}'^2 + \Phi_1\Phi_4 Mv_1^2\right.\right.$$

$$\left.+K\left(\frac{(v_1)_n + (v_1)_{n-1}}{2}'^2\right)\right) \qquad (4.91)$$

The resulting non-linear algebraic equations are then linearized by using Newton's method. For above equations, the $(i+1)th$ iterate can be written as

$$()_n^{(i+1)} = ()_n^{(i)} + \delta()_n^{(i)}, \qquad (4.92)$$

by substitution of (4.92) into (4.86)-(4.91) and ignoring $O(\delta_n^i) \geqslant 2)$, a linear tri-diagonal system is obtained as

$$\delta g_n - \delta h_{n-1} - \frac{1}{2}h(\delta(v_1)_n + \delta(v_1)_{n-1}) = (r_1)_{n-\frac{1}{2}}, \qquad (4.93)$$

$$\delta(v_1)_n - \delta(v_1)_{n-1} - \frac{1}{2}h(\delta(v_2)_n + \delta(v_2)_{n-1}) = (r_2)_{n-\frac{1}{2}}, \qquad (4.94)$$

66

$$\delta\gamma_n - \delta\gamma_{n-1} - \frac{1}{2}h(\delta t_n + \delta t_{n-1}) = (r_3)_{n-\frac{1}{2}}, \tag{4.95}$$

$$\begin{aligned}
(r_4)_{n-\frac{1}{2}} &= (c_1)_n \delta g_j + (c_2)_n \delta g_{n-1} + (c_3)_j \delta(v_1)_n + (c_4)_n \delta(v_1)_{n-1} + (c_4)_n \delta(v_1)_{n-1} + (c_5)_n \delta(v_2)_n \tag{4.96} \\
&\quad + (c_6)_n \delta(v_2)_{n-1} + (c_7)_n \delta\gamma_n + (c_8)_n \delta\gamma_{n-1} + (c_9)_n \delta t_n + (c_{10})_n \delta t_{n-1},
\end{aligned}$$

$$\begin{aligned}
(r_5)_{n-\frac{1}{2}} &= (d_1)_n \delta g_n + (d_2)_n \delta g_{n-1} + (d_3)_n \delta(v_1)_n + (d_4)_n \delta(v_1)_{n-1} + (d_5)_n \delta(v_2)_n \tag{4.97} \\
&\quad + (d_6)_n \delta(v_2)_{n-1} + (d_7)_j \delta\gamma_n + (d_8)_n \delta\gamma_{n-1} + (d_9)_n \delta t_n + (d_{10})_n \delta t_{n-1},
\end{aligned}$$

where

$$(r_1)_{n-\frac{1}{2}} = -g_n + g_{n-1} + \frac{h}{2}((v_1)_n + (v_1)_{n-1}), \tag{4.98}$$

$$(r_2)_{n-\frac{1}{2}} = -(v_1)_n + (v_1)_{n-1} + \frac{h}{2}((v_2)_n + (v_2)_{n-1}), \tag{4.99}$$

$$(r_3)_{n-\frac{1}{2}} = -\gamma_n + \gamma_{n-1} + \frac{h}{2}(t_n + t_{n-1}), \tag{4.100}$$

$$\begin{aligned}
(r_4)_{n-\frac{1}{2}} &= -h\left[-A\left(\frac{(v_1)_n + (v_1)_{n-1}}{2} + \chi\frac{(v_2)_n - (v_2)_{n-1}}{4} \right) + \left(\frac{(v_1)_n + (v_1)_{n-1}}{2} \right)^2 \right. \\
&\quad \left. - \left(\frac{g_n + g_{n-1}}{2} \right)\left(\frac{(v_2)_n + (v_2)_{n-1}}{2} \right) \right] - h\left[-\frac{1}{\Phi_1\Phi_2}\left(\frac{(v_2)_n - (v_2)_{n-1}}{h} \right) \right. \\
&\quad + \beta\left(\left(\frac{g_n + g_{n-1}}{2} \right)^2 \left(\frac{(v_2)_n - (v_2)_{n-1}}{h} \right) - 2\left(\frac{g_n + g_{n-1}}{2} \right)\left(\frac{(v_1)_n + (v_1)_{n-1}}{2} \right) \right. \\
&\quad \left.\left. \left(\frac{(v_2)_n + (v_2)_{n-1}}{2} \right) \right) \right] \qquad\qquad - h\left[\frac{\Phi_4}{\Phi_2}M\left(\frac{(v_1)_n + (v_1)_{n-1}}{2} \right) \right],
\end{aligned}$$

$$(r_5)_{n-\frac{1}{2}} = -h\left[\frac{(t_n - t_{n-1})\left(1 + \frac{1}{\Phi_5}PrNr\right)}{h} + \frac{\Phi_3}{\phi_5}PrA\left(\frac{\gamma_n + \gamma_{n-1}}{2} + \chi\frac{t_n + t_{n-1}}{2}\right)\right]$$
$$-h\frac{\Phi_3}{\Phi_5}Pr\left[\left(\frac{(g_n + g_{n-1})(t_n + t_{n-1})}{4}\right)\left(\frac{(\gamma_j + \gamma_{n-1})((v_1)_n + (v_1)_{n-1})}{4}\right)\right].$$

and boundary conditions are

$$\delta g_0 = 0, \quad (\delta v_1)_0 = 0, \quad \delta t_0 = 0, \quad \delta(v_1)_N = 0, \quad \delta\gamma_N = 0. \tag{4.103}$$

and the resulting matrix form is given in (3.116).

4.4   Verification of numerical results

To ensure the accuracy of our calculations we compare our results to those already available in the literature [26] as the especial case for our study. The test case is MHD flow and heat transfer over permeable stretching sheet with slip conditions. Results are verified for $\beta = 0$, $K = 0$ $\Phi = 0$, $\lambda = 0$, and $Ec = 0$. The comparison shown in Table (4.1) are found to be in excellent agreement. Thus, we are sure about the accuracy of our results.

Table 4.1: Comparison of Skin friction coefficient

Λ	A	M	S	Pr	Nr	Bi	$Andersson$ Results [25]	$T.Hayat$ Results [26]	$Present$ Results
0	0	0	0	0.7	0.2	1.0	1.0000	1.0000	1.0000
0.1							0.8721	0.872082	0.8271
0.2							0.7764	0.776377	0.7764
0.5							0.5912	0.591195	0.5912
0	0.3						-	1.372527	1.3711
	1.5						-	2.0724	2.0748
		1.5	1.0				-	1.756433	1.7560

4.5 Results with Discussion

The numerical results of investigated problem are presented with discussion. The significant effects of physical parameters of Maxwell nanofluid on the velocity, temperature and entropy generation profiles are major part of this discussion. The calculations are performed for Cu and TiO_2 water based nanofluids. In Table (4.2) some values of the skin friction coefficient and the Nusselt number corresponding to flow governing parameters computed at the boundary are tabulated. All of these results are produced for $\beta = 0.3, A = 0.6, M = 0.6, \Phi = 0.2, \Lambda = 0.1, Nr = 0.2, Pr = 6.2, Br = 5, Re = 5, \Omega = 1, S = 0.2, Ec = 0.2$. In graphs, the behavior of $Cu-$water nanofluid is presented in blue color and the behavior of $TiO_2 - water$ is shown by red color.

4.5.1   Influence of Maxwell parameter β

Figures (4.2) and (4.3) demonstrated the effects of β on nanofluid velocity and temperature profile respectively. Computations are performed for $\beta = 0.01, 0.2, 0.3$ for water based non-Newtonian Maxwell nanofluids. The velocity profile tends to decay with increment in β and this caused the reduction in momentum boundary layer. The resistance in fluid is responsible for decay in velocity profile. Whereas with an increment in Maxwell parameter thermal boundary layer expands. Moreover, Figure (4.2) clarifies that thickness of TiO_2-water momentum boundary layer is more than $Cu-$water nanofluid. Whereas with an increment in Maxwell parameter thermal boundary layer expands, and this happens due to increase in elasticity stress parameter. Entropy profile shows cross over point near $\chi = 0.4$, entropy increases before $\chi = 0.4$ and after $\chi = 0.4$ entropy starts decreasing (see Figure (4.4)). It is also observed from Table (4.2) the velocity and temperature gradient for Cu-water and TiO_2-water nanofluids decreases.
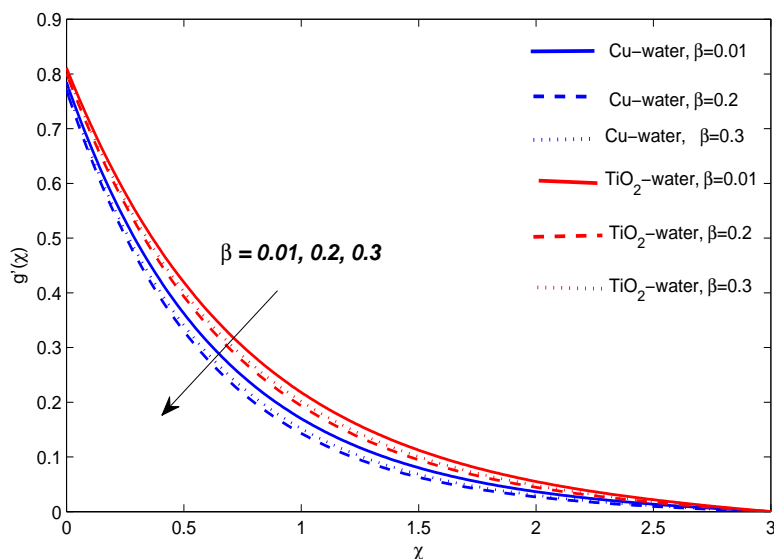
**Figure 4.2:** Velocity distribution against Maxwell parameter β
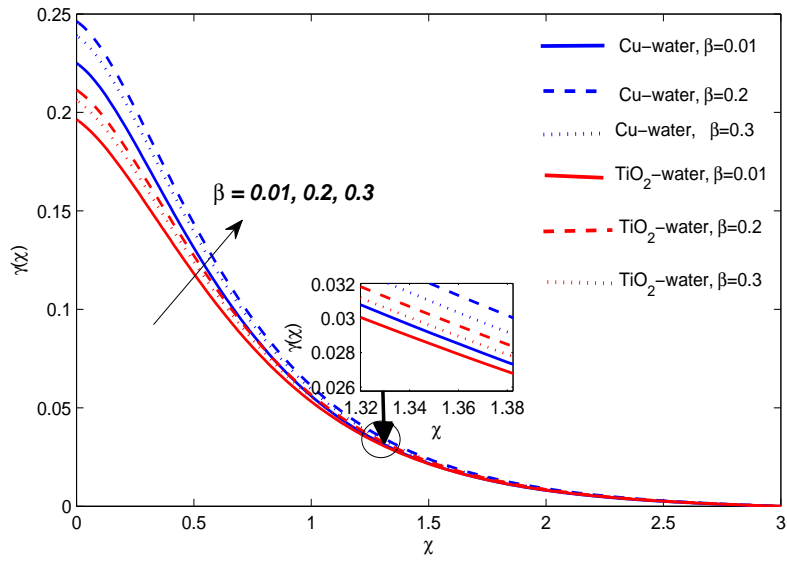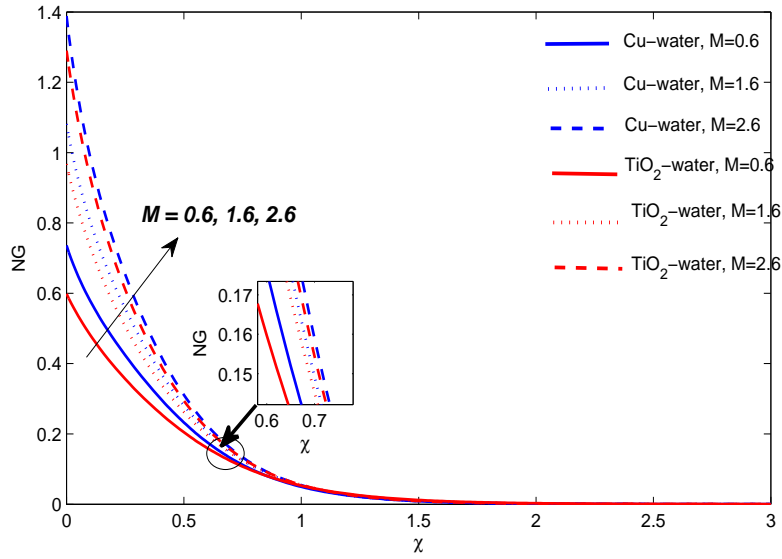
Figure 4.3: Temperature distribution against Maxwell parameter β
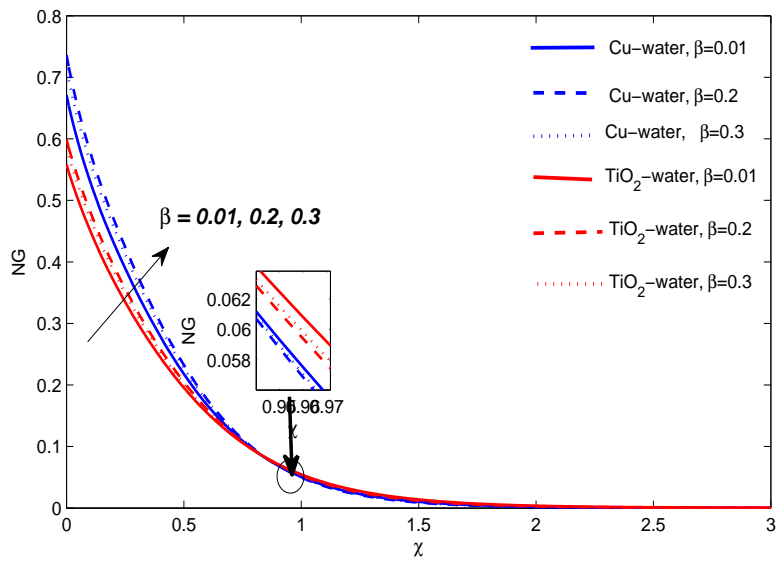
Figure 4.4: Entropy generation against Maxwell parameter β

4.5.2 Influence of unsteadiness parameter A

Figures (4.5) and (4.6) displayed the nature of fluid motion and temperature distribution for Maxwell nanofluid. It is noticed that fluid flows slowly and temperature decreases with increasing values of A. Momentum and thermal boundary layer decreases with increment in A. Temperature profile depicts that the boundary layer thickness of TiO_2-water nanofluid is comparatively more than $Cu-$water nanofluid. Entropy generation profile shows cross over point at $\chi = 0.3$, entropy increases before $\chi = 0.3$ and after $\chi = 0.3$ entropy starts decreasing (see Fig (4.7)). Because boundary layer energy is absorbed due to unsteadiness. Finally, the increase in values of the skin friction and Nusselt numbers is observed for $A = 0.2, 0.6, 1.6$ at the boundary.
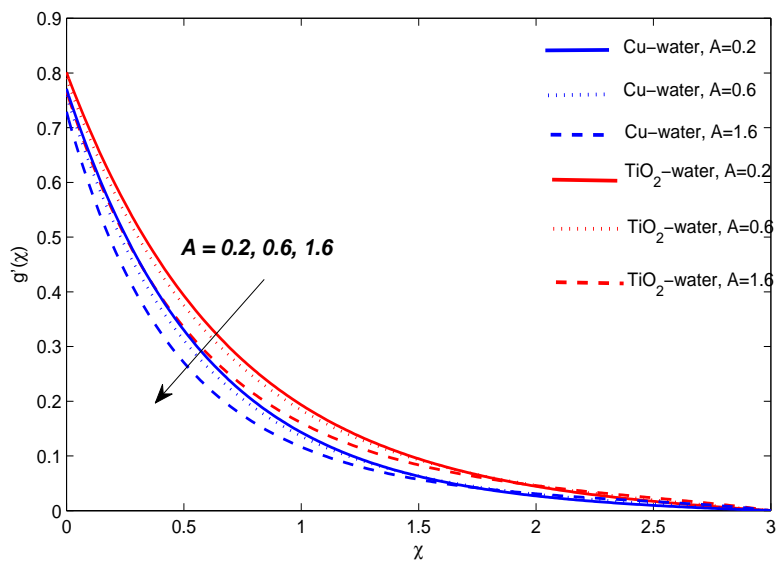
Figure 4.5: Velocity profile for unsteady parameter A

Figure 4.6: Temperature distribution against unsteady parameter A

72
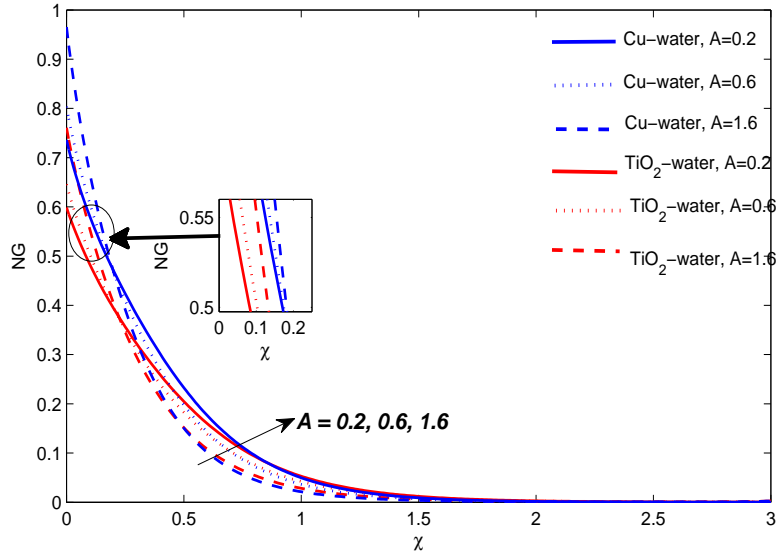
Figure 4.7: Entropy generation against unsteady parameter A.

4.5.3 Influence of magnetic parameter M

The impact of parameter M on the nanofluid motion, temperature and entropy generation profiles are displayed in Figures (4.8)-(4.10) respectively. Computations performed for $M = 0.2, 0.6, 1.6$ showed that the velocity of nanofluids tends to decrease and hence the thickness of momentum boundary layer decreases. The physical reason behind reduction in thickness of momentum boundary layer is that; the Lorentz force which is a resistive force appears when transverse magnetic field is applied and it interacts with the electrically conducting nanofluids. As the strength of applied magnetic field is increased the strength of Lorentz force is also increased and acts opposite to fluid movement within the boundary layer. M is inversely proportional to the density of nanofluid, so increasing M results in a rise of temperature within the boundary layer. Table (4.2) showed that the Nusselt number decreases but the skin friction coefficient increases by variation of M. Entropy of a system rises in

73

this case.
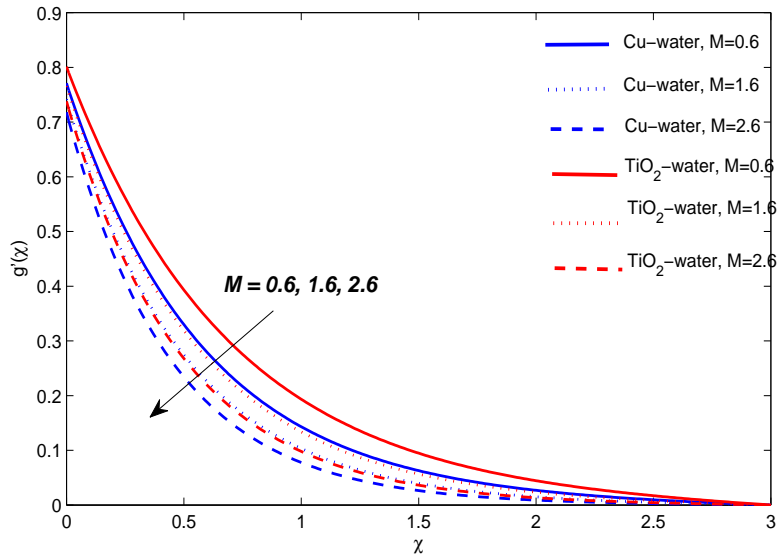
Figure 4.8: Velocity distribution against magnetic parameter M
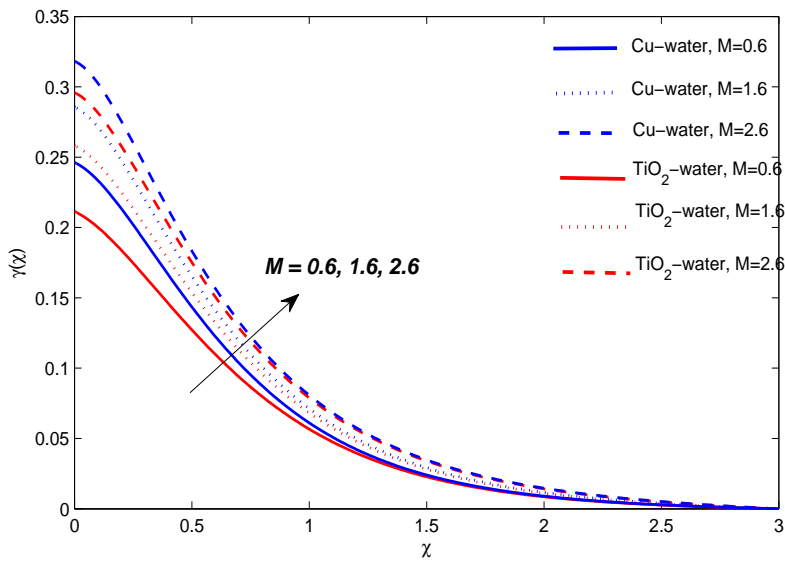
Figure 4.9: Temperature distribution against magnetic parameter M.

Figure 4.10: Entropy generation against magnetic parameter M.

4.5.4 Influence of nanoparticle volume concentration parameter Φ

Figures (4.11) and (4.12) displayed the plots of the fluid motion and temperature distribution corresponding to variation in the parameter ϕ. Velocity is observed to decrease with the increasing parameter ϕ which results in the reduction of the momentum boundary layer thickness. The thinning of the momentum boundary layer is due to heavy nanoparticle volume fraction. In reality the thermal conductivity of nanofluids is enhanced due to increase in volume of nanoparticles. Whereas opposite behavior is observed for temperature profile, the thermal boundary layer expands as the temperature and the thermal conductivity of the nanofluid increases. The increasing trends in both velocity and heat transfer at the boundary corresponding to Φ are shown in Table (4.2). Figure (4.13) depicted the influence of parameter

75

Φ on entropy of system. Increasing the temperature of the nanofluid compels the entropy of system to rise.
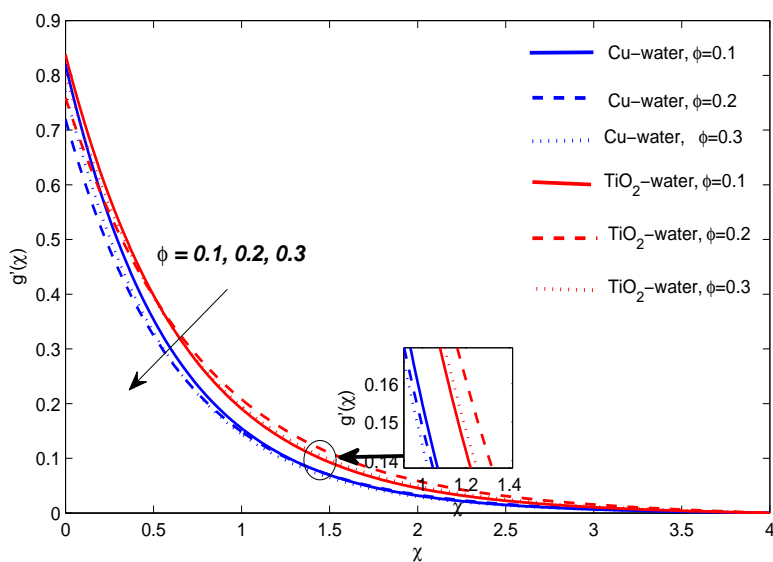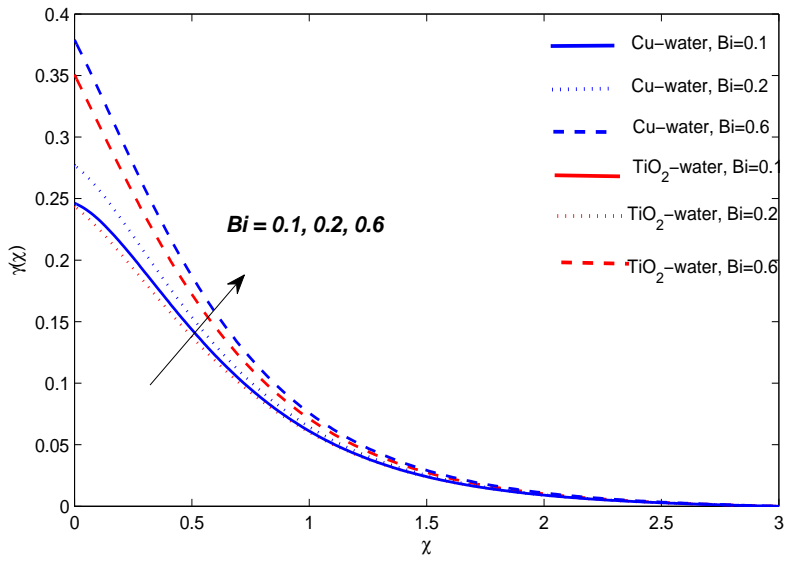

Figure 4.11: Velocity distribution against parameter Φ.
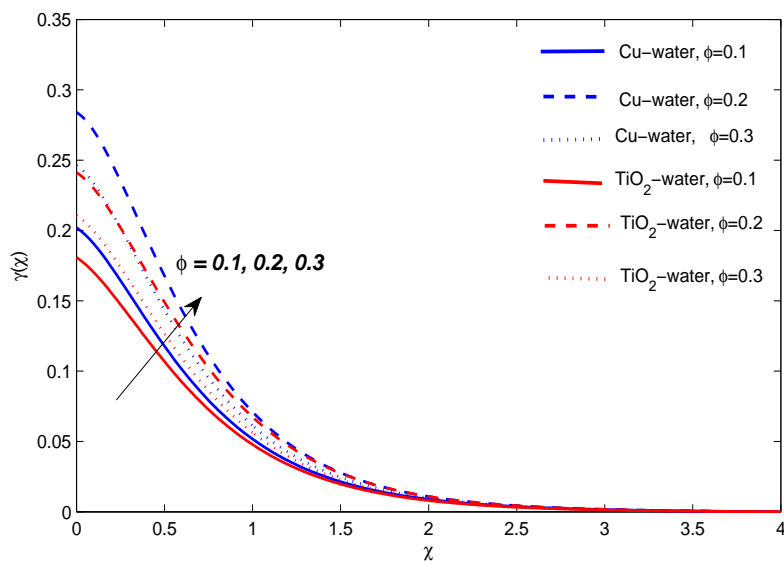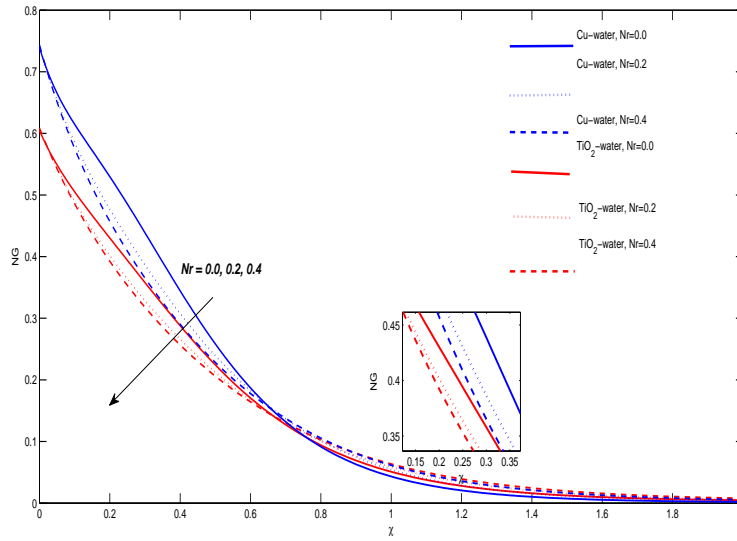

Figure 4.12: Temperature distribution against parameter Φ.
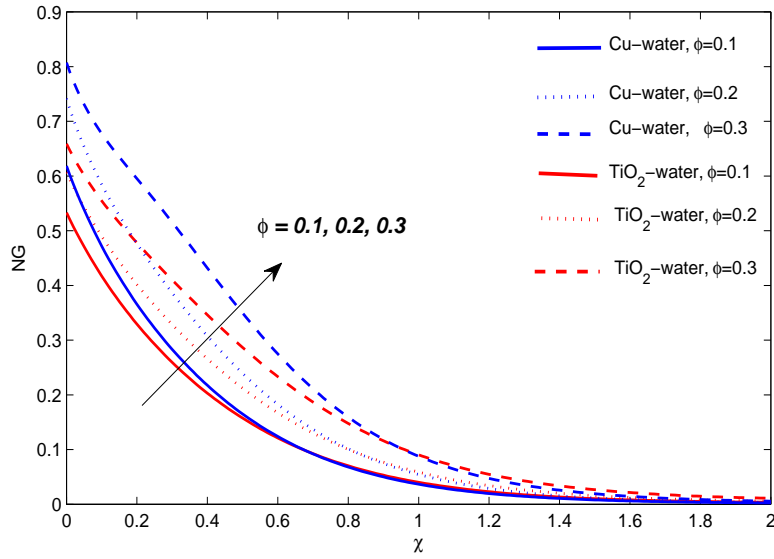
Figure 4.13: Entropy generation against parameter Φ.

4.5.5 Effect of velocity slip Λ

The nature of the fluid motion and temperature are shown for the particular values of slip parameter Λ in Figures (4.14) and (4.15) respectively. Results are calculated for $\Lambda = 0.0, 0.1, 0.2$. Decrease in behavior of velocity profile is observed for the slip parameter Λ, it is obvious because increase in the slipperiness retards the fluid flow which slows down the fluid motion. Temperature of the nanofluid decreases with increase in parameter Λ. Moreover, the thickness of the thermal boundary layer of Cu-water nanofluid is relatively more than the TiO_2-water nanofluid. Here it is important to distinguish that the entropy of the system decreases by increasing the slip parameter as shown in Figure (4.16). The increase in the slip parameter decreases the skin friction coefficient whereas the heat transfer rate increases.
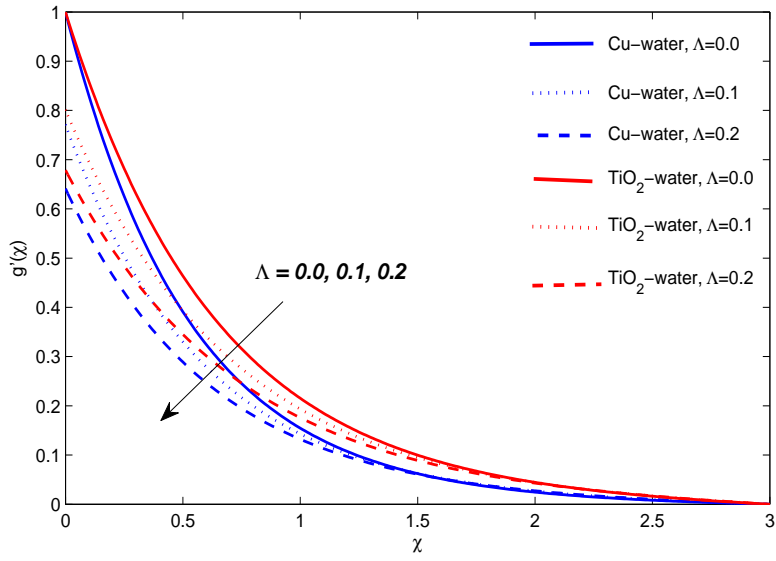
Figure 4.14: Velocity profile for slip effect Λ
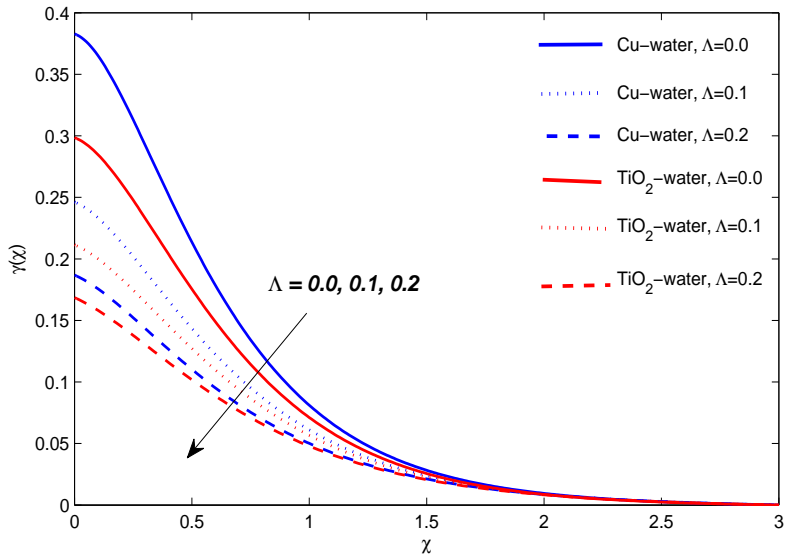
Figure 4.15: Temperature distribution for velocity slip Λ
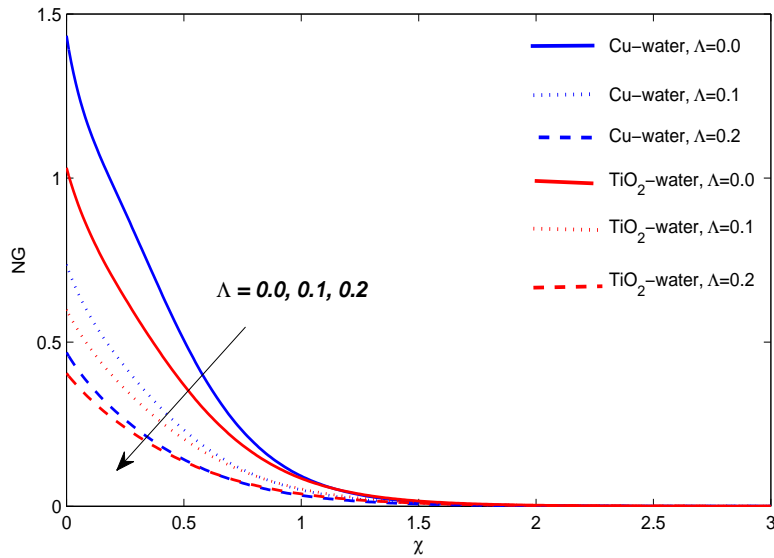
Figure 4.16: Entropy generation against velocity slip parameter Λ

4.5.6   Effect of Biot Number Bi

Figures (4.17) and (4.18) displayed the plots of the nanofluid temperature and entropy generation respectively. Figure (4.17) demonstrated that the temperature of the nanofluids rises due to increase in Biot number. The thermal boundary layer expands due to rise in temperature of the nanofluids. The increase in Biot number causes the larger amount of heat transfer from sheet to the fluid which tends to increase the thermal boundary layer. Whereas, there are no effects of convection parameter (Biot number) on velocity profile of the nanofluid. Entropy in this case increases because of heat transfer.
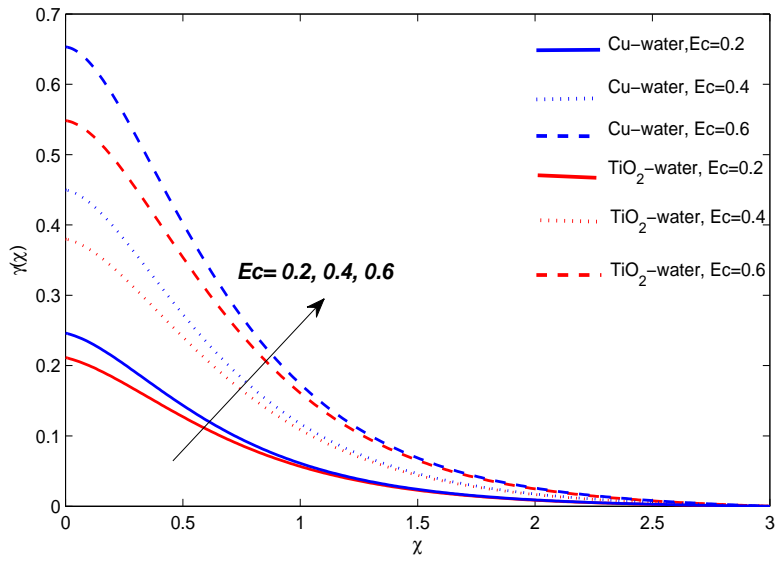
Figure 4.17: Temperature distribution against parameter Bi
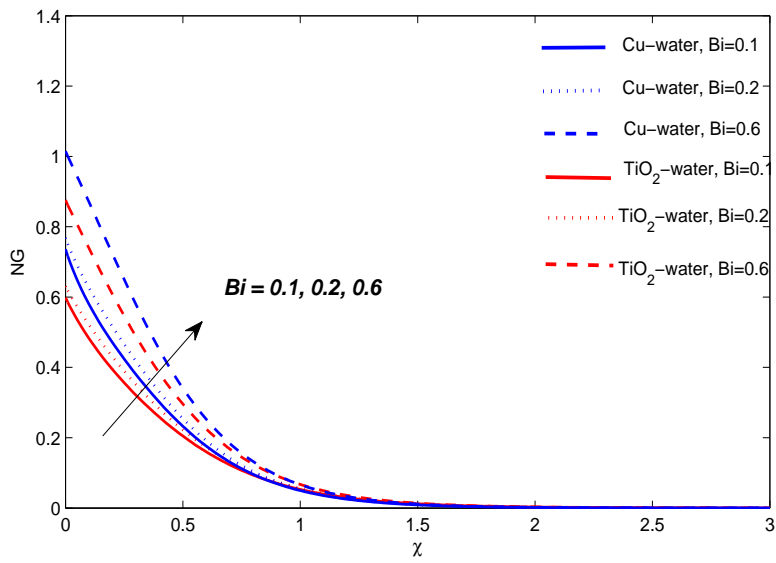
Figure 4.18: Entropy generation against parameter Bi

4.5.7   Influence of thermal radiation parameter Nr

Figure (4.19) presents the effects of thermal radiation parameter Nr on temperature distribution profile of Maxwell nanofluids, which shows that the temperature of nanofluid decreases for ascending values of $Nr = 0.0, 0.2, 0.4$. The thickness of the thermal boundary layer decreases with fall in temperature. Figure (4.20) displays the effect of the parameter Nr on entropy profile for water based nanofluids. There is no change in velocity profile but entropy of nanofluids slows down by variating Nr. Furthermore, it is observed from Table (4.2) that the Nusselt number at the boundary increases for both Cu-water and TiO_2-water whereas the velocity gradient remains constant.
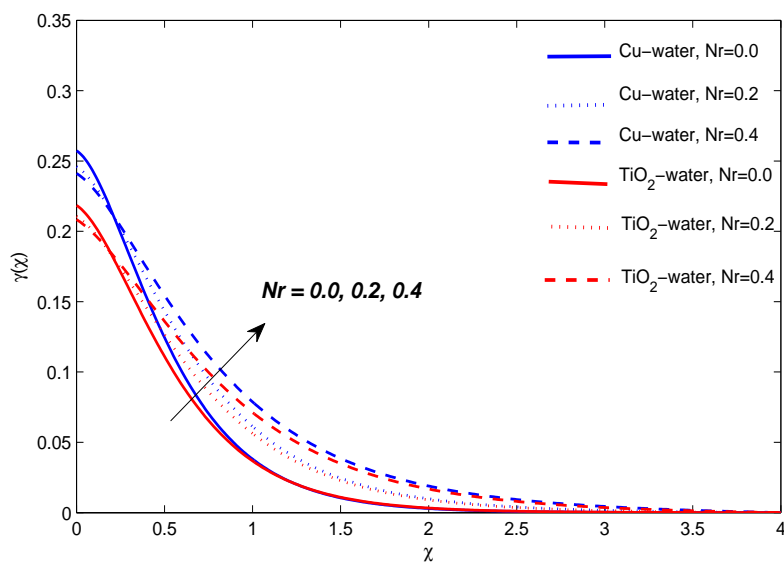
Figure 4.19: Temperature distribution against parameter Nr

Figure 4.20: Entropy profile for Nr

4.5.8 Influence of suction parameter S

Figures (4.21)-(4.23) presented the effect of parameter S on fluid motion, temperature distribution and entropy generation profiles respectively. By increasing the suction parameter the decreasing trend in velocity and temperature profile can be seen and this leads in contraction of momentum and thermal boundary layer thickness. Since applying suction leads to draw the amount of fluid particles into the wall that's why increase in S caused decrease in velocity of the nanofluid. Imposition of the suction on the surface caused reduction in the thermal boundary layer thickness. The velocity and temperature gradient both are observed to be increased for increasing values of S and presented in Table (4.2). By increasing the suction effect the entropy of system is increased.
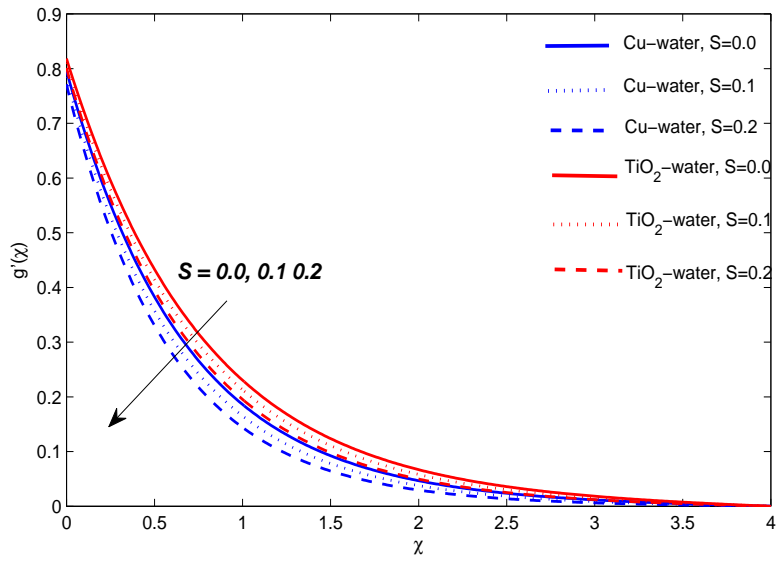
Figure 4.21: Velocity profile for suction parameter S.
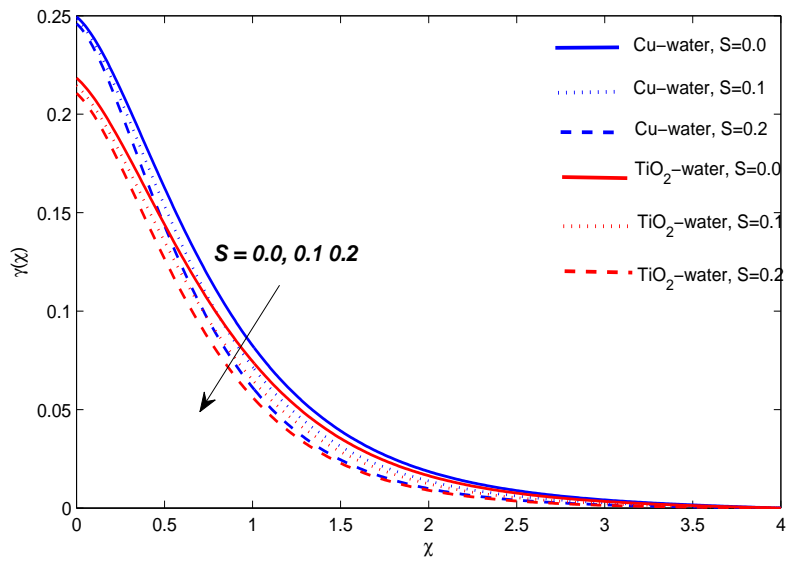
Figure 4.22: Temperature distribution against the parameter S.
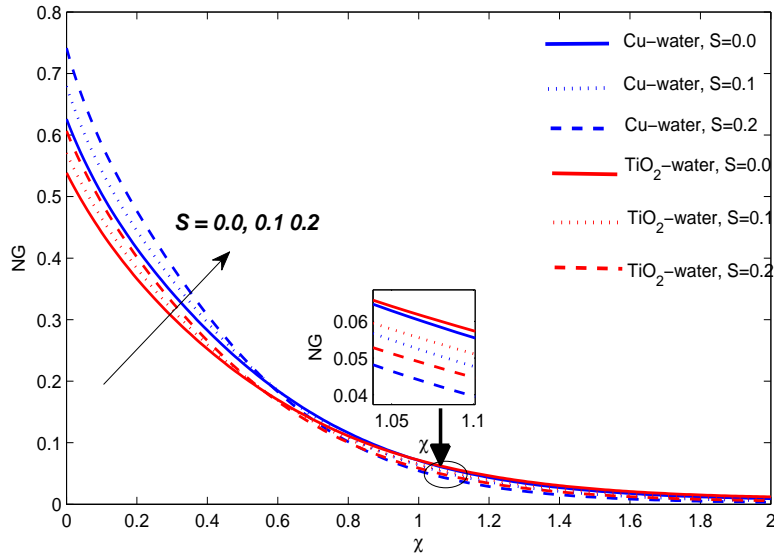
Figure 4.23: Entropy generation distribution against the parameter S.

4.5.9 Effect of Eckert number Ec

Figure (4.24) demonstrates the influence of Eckert Number on temperature distribution. There is increas in temperature profile with rise in values of Eckert number and thermal boundary layer is also enhanced. The physical reason behind this; an increment in dissipation enhances the thermal conductivity of the fluid which also enhances thermal boundary layer. It can be claimed that the presence of viscous dissipation in considered Maxwell nanofluid model increases the temperature distribution and hence the entropy generation, but velocity remains unaltered.

Figure 4.24: Temperature distribution against the parameter Ec.
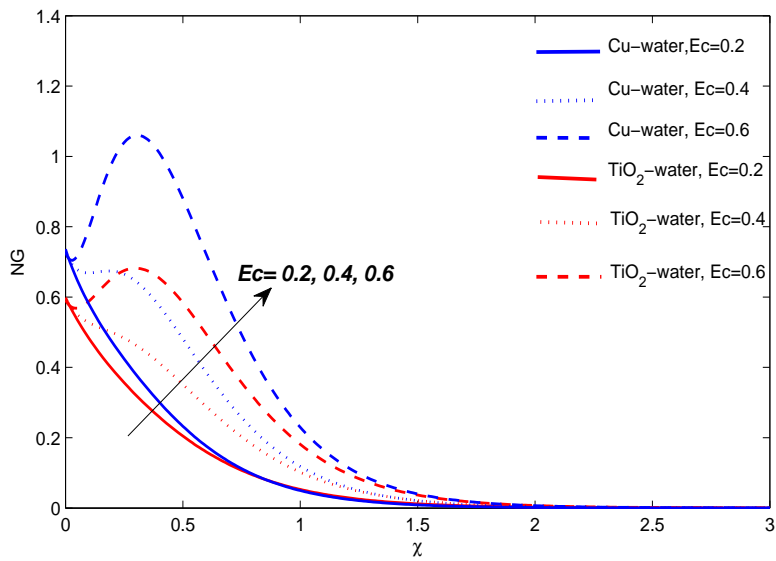
Figure 4.25: Entropy generation against the parameter Ec.

4.5.10 Influence of Brinkmann number Br and Reynolds number Re the entropy generation profiles

Figure (4.26) illustrates the impact of Br on entropy of the system. Entropy of system is found to be increased by increasing the values of Br. Figure (4.27) demonstrated the same behavior of Reynolds number on the entropy of the system. The viscous forces are dominated by the inertial forces at higher Reynolds number, thus the entropy of system increases.
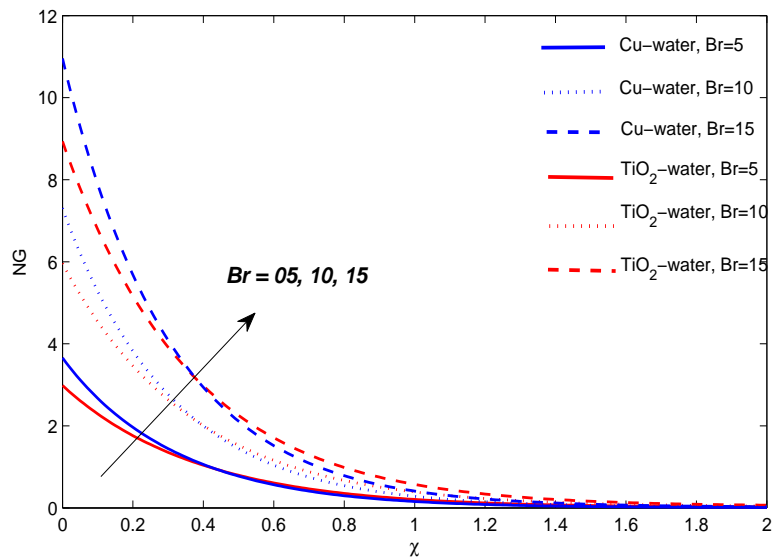
Figure 4.26: Entropy profile for Br.
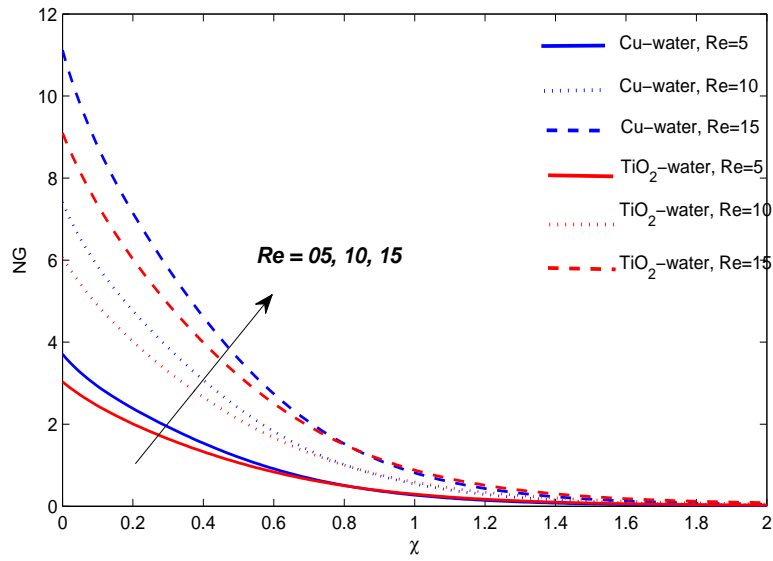
Figure 4.27: Entropy view for Re.

4.5.11 Effect of flow governing parameters on skin friction coefficient and Nusselt Number

The effect of flow governing parameters on the Skin friction (C_f) and the local Nusselt number (Nu_x) is given in the following table.

Table 4.2: Calculation of Skin friction $= C_f Re_x^{\frac{1}{2}}$ and Nusselt number $= N_u Re_x^{\frac{-1}{2}}$ for $Pr = 6.2$

β	A	M	Φ	Λ	Bi	Nr	S	Ec	$C_fRe_x^{\frac{1}{2}}$ $Cu-$ water	$C_fRe_x^{\frac{1}{2}}$ T_iO_2- water	$N_uRe_x^{\frac{-1}{2}}$ $Cu-$ water	$N_uRe_x^{\frac{-1}{2}}$ T_iO_2- water
0.01	0.2	0.6	0.2	0.1	0.1	0.2	0.2	0.2	2.1473	1.8825	0.1625	0.1534
0.2									2.2395	1.9493	0.1595	0.1515
0.3									2.2866	1.9843	0.1580	0.1504
0.3	0.2								2.2866	1.9843	0.1580	0.1504
	0.6								2.4187	2.0923	0.1640	0.1548
	1.6								2.7077	2.3336	0.1727	0.1615
		0.6							2.2866	1.9843	0.1580	0.1504
		1.6							2.5818	2.3433	0.1495	0.1413
		2.6							2.8177	2.6181	0.1426	0.1340
			0.1						1.7950	1.6203	0.1275	0.1246
			0.2						2.2866	1.9843	0.1580	0.1504
			0.3						3.3695	2.9171	0.2456	0.2155
				0.0					3.2574	2.6597	0.1294	0.1339
				0.1					2.2866	1.9843	0.1580	0.1504
				0.2					1.7932	1.6041	0.1704	0.1586
					0.1				2.2866	1.9843	0.1580	0.1504
					0.2				2.2866	1.9843	0.3030	0.2885
					0.6				2.2866	1.9843	0.7808	0.7431
						0.0			2.2866	1.9843	0.1297	0.1241
						0.2			882.2866	1.9843	0.1580	0.1504
						0.4			2.2866	1.9843	0.1854	0.1760
							0.0		2.0355	1.8145	0.1572	0.1490
							0.1		2.1551	1.8957	0.1575	0.1497
							0.2		2.2866	1.9843	0.1580	0.1504

4.6   Conclusion

- Decrease in the velocity profile is observed for an increment in Maxwell and volume fraction parameter.

- Nanoparticles are mainly used in fluids to boost up thermal behavior of fluids. Therefore increase in nanoparticles concentration enhances the temperature of nanofluid and also the thickness of thermal boundary layer.

- The temperature increases with increase in the Eckert number whereas Nusselt numbers decreases.

- Increase in magnetic parameter decreases the momentum boundary layer thickness whereas increases temperature and entropy profile.

- Increase in convection parameter increases temperature profile.

- Increase in thermal radiation increases the temperature and concentration profile.

- As slipperiness retards the fluid flow and causes to decreases the velocity and temperature profile but it is significant to observe that entropy of system decreases by increasing slip parameter.

Chapter 5

Conclusion and Future Work

In this thesis, we have presented the numerical analysis of the non-Newtonian Maxwell nanofluid in presense of slip and convective conditions. Heat transfer is analyzed for unsteady, incompressible two dimensional laminar flow with viscous dissipation and constant thermal conductivity past a porous medium. The governing nonlinear partial differential equations of momentum, energy and entropy generation are changed into ODEs by utilizing a proper similarity transformation. By using the Keller box method, numerical solution of ordinary differential equations is obtained. Distinctive physical parameters are examined, w.r.t dimensionless velocity, temperature and entropy generation profile.

Increase in some parameters such as, β, M and ϕ increases the temperature distribution and also the thickness of thermal boundary layer. This increases the overall entropy of the system. The unsteadiness and velocity slip parameter at the boundary reduces the thickness of the thermal boundary layer and increases the rate of heat transfer at the surface. An increment in viscous dissipation also enhances the thermal conductivity of the nanofluid which also enhances thermal boundary layer

and entropy of system. By increasing values of unsteadiness parameter A, Reynolds number Re, Brinkmann number Br the entropy of system enhances. The entropy of system reduces by variating velocity slip parameter Λ.

This model has bring out valuable outcomes which leads to emphasize on slip effects to reduce the entropy of a system. In future, the present analysis can be extended to include the effects of porosity, variable viscosity and variable thermal conductivity. Furthermore, above mentioned effects can be included in Casson nanofluid model to investigate their effects. There is always an option to conduct experimental studies of such theoretical studies.

Bibliography

[1] S. U. S. Choi, Enhancing thermal conductivity of fluids with nanoparticles, The American Society of Mechanical Engineers, ASME, Fluid Engineering **231**, pp. 99-105, (1995).

[2] J. A. Eastman, S. U. S. Choi, S. Li, L. J. Thompson, and S. Lee, Enhanced thermal conductivity through the development of nanofluids, Fall Meeting of the Materials Research Society, MRS, Boston, USA, (1996).

[3] J. A. Eastman, S. U. S. Choi, S. Li, W. Yu, and L. J. Thompson, Anomalously increased effective thermal conductivities of ethylene glycol based nanofluids containing copper nanoparticles, Applied Physics **78**, pp. 718-720, (2001).

[4] M. Lomascolo, G. Colangelo, M. Milanese, and A. Risi, Review of heat transfer in nanofluids: Conductive, convective and radiative experimental results, Renewable and Sustainable Energy Reviews **43**, pp. 1182-1198 (2015).

[5] B. C. Sakiadis, Boundary layer equations for two dimensional and axisymmetric flow, Boundary layer behavior on continuous solid surfaces, American Institute of Chemical Engineers, pp. 26-28, (1961).

[6] S.Mukhopadhyay, Heat transfer analysis of the unsteady flow of a Maxwell fluid over a stretching surface in the presence of a Heat Source/Sink, Chinese Physical Society **29**, (2012).

[7] L. J. Crane, Flow past a stretching plate, The Journal of Applied Mathematics and Physics (Z.A.M.P)., **21**, pp. 645-647, (1970).

[8] A. Ishak, K. Jafarand, R. Nazar, and I. Pop, MHD stagnation point flow towards a stretching sheet, Statistical Mechanics and its Applications, **388**, pp. 3377-3383, (2009).

[9] J. M. Dorrepaal, Slip flow in converging and diverging channels, Journal of Engineering Mathematics, **27**, pp. 343-356, (1993).

[10] A. Noghrehabadi, R. Pourrajab, and M. Ghalambaz, Effect of partial slip boundary condition on the flow and heat transfer of nanofluids past stretching sheet prescribed constant wall temperature, International Journal of Thermal Sciences, **54**, pp. 253-261, (2012).

[11] R. Sharma, A. Ishak, and I. Pop, Partial slip flow and heat transfer over a stretching sheet in a nanofluid, Mathematical Problems in Engineering, 724547, (2013).

[12] B. K. Chakraborty and H. P. Mazumdar, MHD flow of a newtonian fluid over a stretching sheet: an approximate solution, Approximation Theory and its Applications, **16**, pp. 32-41, (2000).

[13] A. Aziz, W. Jamshed and T. Aziz, Mathematical model for thermal and entropy analysis of thermal solar collectors by using maxwell nanofluids with slip

conditions, thermal radiation and variable thermal conductivity, Open Physics, **16**, pp. 123-136, (2017).

[14] P. Naphon, Second-law analysis on the heat transfer of the horizontal concentric tube heat exchanger, International Communications in Heat and Mass Transfer **33**, pp. 1029-1041, (2006).

[15] A. Bejan, Entropy Generation Minimization: The method of thermodynamic optimization of finite-size systems and finite-time processes, CRC Press, (1996).

[16] O. Mahian, S. Mahmud, S.Z. Heris, Analysis of entropy generation between co-rotating cylinders using nanofluids, Energy, **44**, pp. 438-446, (2012).

[17] R. W. Fox and A. T. McDonald's, *Introduction to fluid mechanics*, John Wiley and Sons, Inc., **5**, (2004).

[18] L. Prandtl, On fluid motions with very small friction, Verhldg, **3**, pp. 484-491, (1904).

[19] H. C. Brinkman, The viscosity of concentrated suspensions and solutions, The Journal of Chemical Physics, **20** (1952).

[20] K. Khanafer, K. Vafai and M. Lightstone, Buoyancy-driven heat transfer enhancement in a two-dimensional enclosure utilizing nanofluids. International Journal of Heat and Mass Transfer, **46** pp. 3639-3653, (2003).

[21] M. S. Abel, J. V. Tawade , M. Nandeppanavar, MHD flow and heat transfer for the upper-convected Maxwell fluid over a stretching sheet, Meccanica., **47**, pp. 385-393, (2012).

[22] H. B. Keller, A New Difference Scheme for Parabolic Problems, Hubbard, B., Ed., Numerical Solutions of Partial Differential Equations, Acad. Press, New York., **2**, pp. 327-350 (1971).

[23] M. Q. Brewster, Thermal radiative transfer and properties, John Wiley and Sons, (1992).

[24] S. Das, S. Chakraborty, R. N. Jana, O. D. Makinde , Entropy analysis of unsteady magneto-nanofluid flow past accelerating stretching sheet with convective boundary condition, Applied Mathematics and Mechanics, **36**, pp. 1593-1610, (2015).

[25] H. I. Andersson, Slip flow past a stretching surface, Acta Mechanica **158**; pp. 121-125, (2002).

[26] T. Hayat, M. Qasim, S. Mesloub MHD flow and heat transfer over permeable stretching sheet with slip conditions International Journal for Numerical Methods in Fluids, **66**, pp. 963-975, (2011).